Suppressing Farnesyl Diphosphate Synthase Alters Chloroplast Development and Triggers Sterol-Dependent Induction of Jasmonate- and Fe-Related Responses[1][OPEN]

David Manzano*, Paola Andrade[2], Daniel Caudepón, Teresa Altabella, Montserrat Arró, and Albert Ferrer

Plant Metabolism and Metabolic Engineering Program, Centre for Research in Agricultural Genomics, CSIC-IRTA-UAB-UB, Campus UAB, Bellaterra (Cerdanyola del Vallès), Barcelona, Spain (D.M., P.A., D.C., T.A., M.A., A.F.); and Department of Biochemistry and Molecular Biology (D.M., P.A., D.C., M.A., A.F.) and Plant Physiology Unit (T.A.), Faculty of Pharmacy, University of Barcelona, Barcelona, Spain

ORCID IDs: 0000-0002-5483-7223 (D.M.); 0000-0002-6915-5823 (T.A.); 0000-0002-0741-2388 (A.F.).

Farnesyl diphosphate synthase (FPS) catalyzes the synthesis of farnesyl diphosphate from isopentenyl diphosphate and dimethylallyl diphosphate. Arabidopsis (*Arabidopsis thaliana*) contains two genes (*FPS1* and *FPS2*) encoding FPS. Single *fps1* and *fps2* knockout mutants are phenotypically indistinguishable from wild-type plants, while *fps1/fps2* double mutants are embryo lethal. To assess the effect of FPS down-regulation at postembryonic developmental stages, we generated Arabidopsis conditional knockdown mutants expressing artificial microRNAs devised to simultaneously silence both *FPS* genes. Induction of silencing from germination rapidly caused chlorosis and a strong developmental phenotype that led to seedling lethality. However, silencing of FPS after seed germination resulted in a slight developmental delay only, although leaves and cotyledons continued to show chlorosis and altered chloroplasts. Metabolomic analyses also revealed drastic changes in the profile of sterols, ubiquinones, and plastidial isoprenoids. RNA sequencing and reverse transcription-quantitative polymerase chain reaction transcriptomic analysis showed that a reduction in FPS activity levels triggers the misregulation of genes involved in biotic and abiotic stress responses, the most prominent one being the rapid induction of a set of genes related to the jasmonic acid pathway. Down-regulation of FPS also triggered an iron-deficiency transcriptional response that is consistent with the iron-deficient phenotype observed in FPS-silenced plants. The specific inhibition of the sterol biosynthesis pathway by chemical and genetic blockage mimicked these transcriptional responses, indicating that sterol depletion is the primary cause of the observed alterations. Our results highlight the importance of sterol homeostasis for normal chloroplast development and function and reveal important clues about how isoprenoid and sterol metabolism is integrated within plant physiology and development.

Isoprenoids are the largest class of all known natural products in living organisms, with tens of thousands of different compounds. In plants, isoprenoids perform essential biological functions, including maintenance of proper membrane structure and function (sterols), electron transport (ubiquinones and plastoquinones), post-translational protein modification (dolichols serving as glycosylation cofactors and prenyl groups), photosynthesis (chlorophylls and carotenoids), and regulation of growth and development (abscisic acid, brassinosteroids, cytokinins, and GAs [Croteau et al., 2000] and strigolactones [Al-Babili and Bouwmeester, 2015]). A large number of isoprenoids also play prominent roles as mediators of interactions between plants and their environment, including a variety of defense responses against biotic and abiotic stresses (Tholl and Lee, 2011). In fact, there is hardly any aspect of plant growth, development, and reproduction not relying on isoprenoids or isoprenoid-derived compounds. In addition, many plant isoprenoids are of great economic importance because of their wide range of industrial and agricultural applications (Bohlmann and Keeling, 2008; George et al., 2015).

All isoprenoids derive from the five-carbon (C_5) building blocks isopentenyl diphosphate (IPP) and its isomer dimethylallyl diphosphate (DMAPP). These precursors can be synthesized through two distinct pathways: the mevalonic acid (MVA) pathway and the 2-*C*-methyl-D-erythritol 4-phosphate (MEP) pathway (for review, see Hemmerlin et al., 2012). In contrast to most organisms, plants use both pathways to form IPP and DMAPP, which operate independently and are

[1] This work was supported by the Spanish Government (grant nos. BIO2009–06984 and AGL2013–43522-R to A.F.) and the Generalitat de Catalunya (grant no. 2014SGR–1434).

[2] Present address: Biotechnology Laboratory, Instituto de Investigaciones Agropecuarias, La Platina Research Station, Avenida Santa Rosa 11610, La Pintana 8831314, Santiago, Chile.

* Address correspondence to david.manzano@ub.edu.

The author responsible for distribution of materials integral to the findings presented in this article in accordance with the policy described in the Instructions for Authors (www.plantphysiol.org) is: David Manzano (david.manzano@ub.edu).

D.M. and A.F. conceived and designed the research; D.M., P.A., D.C., T.A., and M.A. performed the research; D.M. and A.F. performed data analysis, collection, and interpretation and wrote the article.

[OPEN] Articles can be viewed without a subscription.

www.plantphysiol.org/cgi/doi/10.1104/pp.16.00431

located in different cell compartments (Fig. 1A). The MVA pathway operates in the cytosol/endoplasmic reticulum (ER), while the MEP pathway localizes into plastids (Vranová et al., 2013). Both pathways are essential for plant viability (Rodríguez-Concepción et al., 2004). Then, different prenyltransferases catalyze a series of sequential head-to-tail condensations of IPP with DMAPP and the resulting allylic diphosphates to produce linear prenyl diphosphates of increasing chain length. Among these are the short-chain trans- or (*E*)-prenyl diphosphates, geranyl diphosphate (GPP; C_{10}), farnesyl diphosphate (FPP; C_{15}) geranylgeranyl diphosphate (GGPP; C_{20}), and geranylfarnesyl diphosphate (GFPP; C_{25}; Fig. 1A), so called because of the stereochemistry of the double bond established between IPP and the allylic substrates (Wang and Ohnuma, 2000; Vandermoten et al., 2009; Nagel et al., 2015). These linear prenyl diphosphates are further metabolized by terpene synthases, leading to the large variety of cyclic and acyclic terpenoid carbon skeletons found in plants, which are subsequently decorated by oxidation, reduction, isomerization, conjugation, or other secondary transformations to produce the myriad different isoprenoids found in plants (Chen et al., 2011; Kumari et al., 2013).

FPS (EC 2.5.1.10) catalyzes the condensation of MVA-derived IPP and DMAPP to form GPP, the allylic intermediate that undergoes a second condensation reaction with IPP to produce FPP (Poulter, 2006). Cytosolic FPP serves as a common precursor of sterols, triterpenes and brassinosteroids, dolichols and polyprenols, sesquiterpenes, and the farnesyl moiety of heme groups and prenylated proteins (Fig. 1A; Vranová et al., 2013). FPP formed in the mitochondria from MVA-derived IPP and

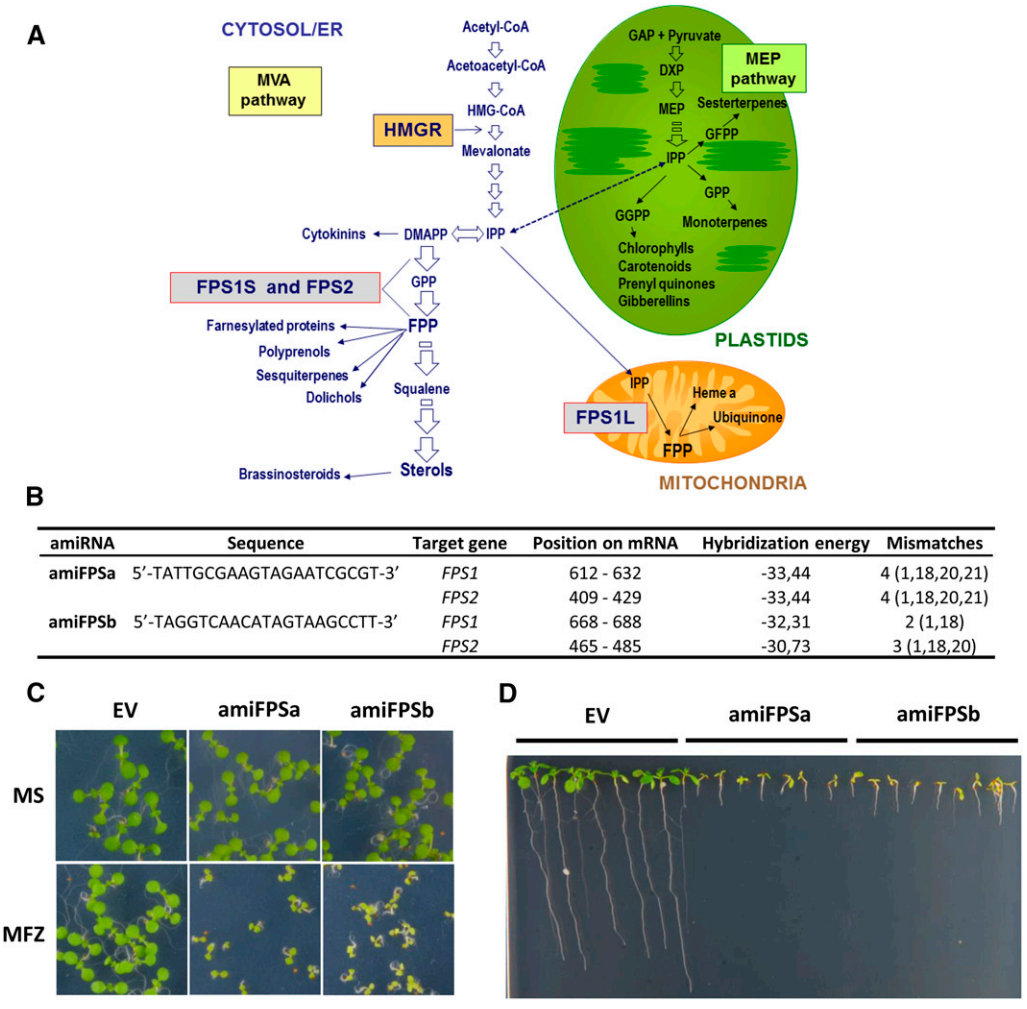

amiRNA	Sequence	Target gene	Position on mRNA	Hybridization energy	Mismatches
amiFPSa	5′-TATTGCGAAGTAGAATCGCGT-3′	*FPS1*	612 - 632	-33,44	4 (1,18,20,21)
		FPS2	409 - 429	-33,44	4 (1,18,20,21)
amiFPSb	5′-TAGGTCAACATAGTAAGCCTT-3′	*FPS1*	668 - 688	-32,31	2 (1,18)
		FPS2	465 - 485	-30,73	3 (1,18,20)

Figure 1. Silencing of Arabidopsis *FPS* gene expression using amiRNA technology alters plant shoot and root phenotypes. A, Simplified scheme of the isoprenoid biosynthetic pathways. The reactions catalyzed by 3-hydroxy-3-methylglutaryl coenzyme A reductase (HMGR) and farnesyl diphosphate synthase (FPS) are indicated. DXP, 1-Deoxy-D-xylulose-5-phosphate; GAP, glyceraldehyde 3-phosphate. B, Main features of the amiRNAs designed for *FPS1* and *FPS2* gene silencing. C, Shoot phenotypes of 8-d-old EV, amiFPSa, and amiFPSb seedlings grown on MS medium (top images) and MS medium supplemented with 30 μM MFZ (bottom images). D, Root phenotypes of 10-d-old EV, amiFPSa, and amiFPSb seedlings grown on MS medium supplemented with 30 μM MFZ.

DMAPP serves as a precursor of ubiquinones (Disch et al., 1998). On the contrary, GPP, GGPP, and GFPP are mostly produced in plastids from MEP-derived IPP and DMAPP by GPP synthase, GGPP synthase, and GFPP synthase, respectively. GPP is the precursor of monoterpenes, whereas GGPP is utilized for the biosynthesis of photosynthetic pigments such as chlorophylls and carotenoids, plastoquinones and other plastidial prenyl quinones, diterpenes and GAs via oxidative carotenoid cleavage, strigolactones and abscisic acid, and finally for protein geranylgeranylation (Vranová et al., 2013; Al-Babili and Bouwmeester, 2015; Huchelmann et al., 2016). GFPP is the suggested precursor of sesterterpenes (Fig. 1A; Nagel et al., 2015). Although it is widely accepted that isoprenoids of cytosolic and plastidial origin are mostly formed from physically segregated pools of linear prenyl diphosphates, it is also well documented that, under certain growth conditions and/or in specific plant tissues and species, there is a limited exchange of precursors between the cytosol and plastidial isoprenoid pathways (Vranová et al., 2012; Opitz et al., 2014). IPP, DMAPP, GPP, and FPP are considered the most plausible intermediates to be transported across the plastidial membranes (Soler et al., 1993; Bick and Lange, 2003; Flügge and Gao, 2005), although the precise mechanisms by which this exchange occurs and is regulated, the identity of the putative prenyl phosphate transporters, and the real capacity of plants to exchange intermediates between these compartments remain to be established (Opitz et al., 2014).

Arabidopsis (*Arabidopsis thaliana*) contains two genes encoding FPS, namely *FPS1* (At5g47770) and *FPS2* (At4g17190; Cunillera et al., 1996). *FPS1* encodes isoforms FPS1L and FPS1S, which differ by an N-terminal extension of 41 amino acids that targets FPS1L into mitochondria (Cunillera et al., 1997; Manzano et al., 2006), whereas FPS1S, like FPS2, localizes to the cytosol (Fig. 1A; Keim et al., 2012). The characterization of Arabidopsis mutants with either gain or loss of function of specific *FPS* genes revealed that *FPS1* and *FPS2* have highly overlapping but not completely redundant functions in isoprenoid biosynthesis. Overexpression of FPS1L or FPS1S causes a cell death/senescence-like phenotype due to a metabolic imbalance that impairs cytokinin biosynthesis (Masferrer et al., 2002; Manzano et al., 2006), whereas overexpression of FPS2 has no apparent detrimental effect on plant growth and development (Bhatia et al., 2015). On the other hand, *fps1* and *fps2* single knockout mutants are almost indistinguishable from wild-type plants, which is in sharp contrast with the embryo lethality of the *fps1/fps2* double mutant (Closa et al., 2010). That work and several other studies have demonstrated that normal functioning of the isoprenoid pathway in the cytosol is indispensable for plant viability. Genetic lesions affecting different enzymatic steps of this biosynthetic pathway result in male gamete-impaired genetic transmission or early embryonic or postembryonic developmental arrest (Schrick et al., 2000, 2002; Kim et al., 2005; Babiychuk et al., 2008; Suzuki et al., 2009; Carland et al., 2010; Closa et al., 2010; Ishiguro et al., 2010; Jin et al., 2012). These lethal phenotypes have been attributed primarily to the depletion of sterol levels, the major MVA-derived end products.

Plant sterols consist of a mixture of three major species, namely β-sitosterol (the most abundant one), stigmasterol, and campesterol, and a variety of minor sterols that are biosynthetic precursors of the main sterols (Schaller, 2003; Benveniste, 2004). β-Sitosterol, stigmasterol, and campesterol are the bulk membrane sterols (Hartmann-Bouillon and Benveniste, 1987), and campesterol is also a precursor of the brassinosteroids (Fujioka and Yokota, 2003). Sterols are integral components of plant cell membranes that are found predominantly in the plasma membrane and in a much lower amount in the tonoplast, ER, mitochondria (Hartmann, 1998; Horvath and Daum, 2013), and the outer membrane of chloroplasts (Moeller and Mudd, 1982; Hartmann-Bouillon and Benveniste, 1987; Lenucci et al., 2012). In addition to this key structural role, sterols also play pivotal roles in embryonic, vascular, and stomatal patterning (Jang et al., 2000; Carland et al., 2002; Qian et al., 2013), cell division, expansion, and polarity (He et al., 2003; Men et al., 2008), hormonal regulation (Souter et al., 2002; Kim et al., 2010), vacuole trafficking (Li et al., 2015), and cell wall formation (Schrick et al., 2012). Some recent reports also point toward a role for sterols in proper plastid development (Babiychuk et al., 2008; Kim et al., 2010; Gas-Pascual et al., 2015). As key components of cell membranes, sterols are dynamic modulators of their biophysical properties, so that changes in the composition of sterols affect membrane fluidity and permeability (Roche et al., 2008; Grosjean et al., 2015) and, therefore, modulate the activity of membrane-bound proteins (Carruthers and Melchoir, 1986; Cooke and Burden, 1990; Grandmougin-Ferjani et al., 1997) and the plant adaptive responses to different types of abiotic and biotic stress, including tolerance to thermal stress (Hugly et al., 1990; Beck et al., 2007; Senthil-Kumar et al., 2013), drought (Posé et al., 2009; Kumar et al., 2015), metal ions (Urbany et al., 2013; Wagatsuma et al., 2015), and hydrogen peroxide (Wang et al., 2012a), and to bacterial and fungal pathogens (Griebel and Zeier, 2010; Wang et al., 2012b; Kopischke et al., 2013).

The embryo-lethal phenotype of the Arabidopsis *fps1/fps2* double knockout mutants makes it very difficult to assess the biological role of FPP biosynthesis in postembryonic plant development. To overcome this drawback, we generated conditional knockdown Arabidopsis mutants using a chemically inducible artificial microRNA (amiRNA)-based gene-silencing approach to down-regulate *FPS* gene expression. We report here the results of the phenotypic, metabolomic, and transcriptomic analyses of these mutants. Upon FPS silencing, plants develop a chlorotic phenotype associated with important alterations in chloroplast development and a marked alteration in the profile of the major cytosolic, mitochondrial, and plastidial

isoprenoids. In addition, we demonstrate that FPS down-regulation and the concomitant depletion of bulk membrane sterols trigger an early misregulation of genes involved in stress responses, the misregulation of genes related to the jasmonic acid (JA) pathway and the maintenance of cellular iron (Fe) homeostasis being particularly remarkable. This transcriptional response is mimicked by the specific inhibition of the sterol biosynthesis pathway, suggesting that even though FPP serves as a precursor of a number of essential isoprenoid end products, sterol depletion is the primary cause of the observed alterations.

RESULTS

Characterization of Conditional Arabidopsis FPS Knockdown Mutants

Arabidopsis mutants harboring a single functional *FPS* gene show only slight phenotypic alterations that appear during the early stages of development, whereas simultaneous knockout of both *FPS* genes is embryo lethal (Closa et al., 2010). This makes it extremely difficult to assess the biological function of FPS beyond this stage of development. To overcome this limitation, we generated conditional Arabidopsis *FPS* knockdown mutant lines by combining an ecdysone-inducible promoter (Padidam et al., 2003) with the amiRNA technology (Schwab et al., 2006). The Web MicroRNA Designer 3 tool (http://wmd3.weigelworld.org/cgi-bin/webapp.cgi) was used to generate a list of candidate amiRNAs specifically devised to simultaneously silence both *FPS* genes. Two amiRNAs, referred to as amiFPSa and amiFPSb, were chosen from the top rank list. The sequences of these amiRNAs, their positions on the FPS1 and FPS2 mRNA sequences, their hybridization energy, and the numbers and positions of the mismatches are shown in Figure 1B. The sequences containing the amiFPSa and amiFPSb precursors were cloned into the pB110-Red-284 binary vector harboring the ecdysone receptor-based inducible gene expression system (Padidam et al., 2003; Dietrich et al., 2008) and a DsRed constitutive expression cassette allowing for the identification of transgenic red fluorescent seeds. Arabidopsis Columbia-0 (Col-0) plants were then transformed using the *Agrobacterium tumefaciens*-mediated floral dip method (Clough and Bent, 1998). Based on the segregation analysis of the fluorescent seed trait, several independent T3 homozygous lines harboring the amiFPS precursor constructs were generated, and one line for each amiRNA was selected for further characterization. Plants of the amiFPSa and amiFPSb selected lines grown on Murashige and Skoog (MS) medium were indistinguishable from Arabidopsis Col-0 plants transformed with the pB110-Red-284 vector lacking the pre-amiRNA construct, further referred to as empty vector (EV) plants. However, plants germinated in the presence of 30 μM methoxyfenozide (MFZ), the ecdysone receptor agonist (Padidam et al., 2003; Koo et al., 2004), displayed a strong detrimental phenotype. Plants showed a severe size reduction of roots and the aerial part, chlorosis in the cotyledons, and failed to develop true leaves (Fig. 1, C and D), which ultimately caused them to die. None of these effects was observed in EV plants treated with MFZ (Fig. 1, C and D) or amiFPS and EV plants grown on MS medium (Fig. 1C).

The severe developmental phenotype observed when amiFPS plants were germinated in the presence of MFZ made it impossible to distinguish between the effects specifically attributable to the silencing of FPS and those due to the developmental delay of FPS-silenced plants compared with control plants. To overcome this constraint, amiFPSa and amiFPSb plants were first grown for 3 d on MS medium and then transferred to MS medium supplemented with MFZ. Under these conditions, degreening symptoms started to appear in cotyledons between 2 and 3 d after the induction of silencing and became evenly spread over the whole cotyledons and leaves at 5 d after induction (Fig. 2A). Interestingly, the first pair of true leaves showed only a slight reduction in size. Thus, the developmental stage of amiFPS plants was considered comparable to that of the control plants (Fig. 2A), and these experimental conditions were selected to further characterize the response of plants to FPS silencing.

FPS gene expression analysis in silenced amiFPSa and amiFPSb plants revealed that FPS1 mRNA levels were reduced to 21% and 16%, respectively, of those in the EV plants treated with MFZ, while FPS2 mRNA levels were reduced to 26% and 35%, respectively (Fig. 2B). Such a drastic reduction of FPS transcript levels confirmed that both amiRNAs were highly effective in silencing *FPS* gene expression, although with a slightly different specificity toward their mRNA targets. Protein-blot analysis using anti-FPS antibodies (Manzano et al., 2006) and FPS activity measurements demonstrated a concomitant reduction of total FPS protein (Fig. 2C) and enzyme activity, which in amiFPSa and amiFPSb plants treated with MFZ dropped to below 40% and 50% of the activity in the control plants, respectively (Fig. 2D). On the contrary, no significant differences in FPS mRNA, protein, and enzyme activity levels were detected in amiFPS plants grown on MS medium compared with EV plants grown on MS medium or MS medium supplemented with MFZ (Fig. 2, B–D). Constitutive overexpression of isoform FPS1S in amiFPSa plants harboring a *35S::FPS1S* transgene (Masferrer et al., 2002; Supplemental Fig. S1A) fully complemented the phenotype of MFZ-treated amiFPSa plants (Supplemental Fig. S1B), demonstrating that the phenotype displayed by amiFPS plants upon treatment with MFZ was specifically due to down-regulation of FPS activity and not to undesired off-target gene-silencing effects or to the inducible expression system used (compare EV results in Fig. 2).

Down-Regulation of FPS Leads to Altered Levels of Major MVA-Derived Isoprenoids and Triggers Posttranscriptional Up-Regulation of HMGR Activity

Quantitative analysis of sterols by gas chromatography-mass spectrometry in amiFPSa, amiFPSb, and EV plants

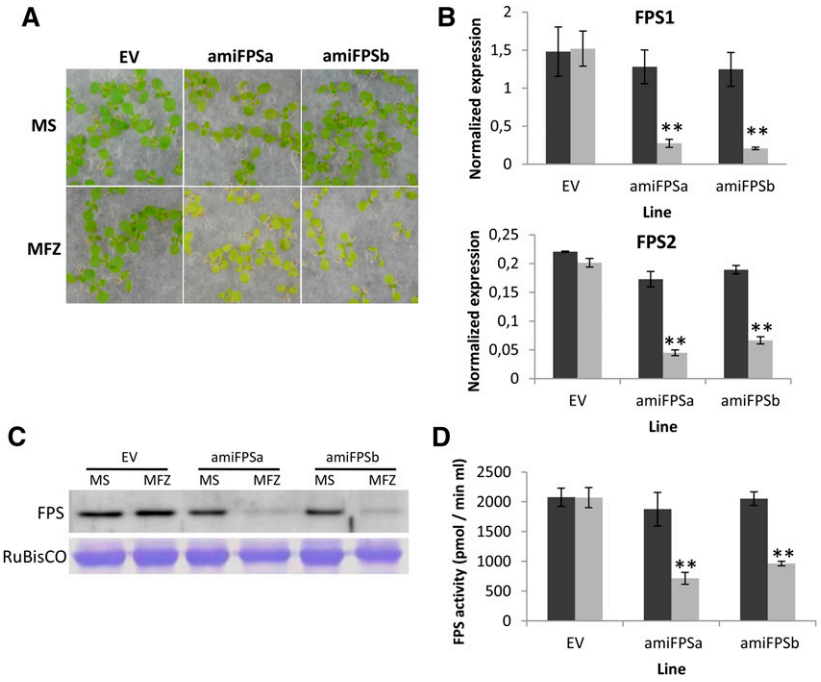

Figure 2. Expression of amiFPSa and amiFPSb leads to reduced levels of FPS mRNA, protein, and enzyme activity. A, Phenotypes of EV, amiFPSa, and amiFPSb seedlings grown for 8 d on MS medium (top images) or 3 d on MS medium and 5 d on MS medium supplemented with 30 μM MFZ (bottom images). B, RT-qPCR analysis of *FPS1* and *FPS2* transcripts using RNA from EV, amiFPSa, and amiFPSb seedlings grown on MS medium (black bars) or 3 d on MS medium and 5 d on MS medium supplemented with 30 μM MFZ (gray bars). Transcript levels were normalized relative to the mRNA levels of the *PP2AA3* gene. C, Western-blot analysis of FPS protein (top) and Coomassie Brilliant Blue-stained large subunit of Rubisco (bottom) in extracts of EV, amiFPSa, and amiFPSb plants grown as indicated above. Membranes show the results of a representative experiment. D, FPS activity in the same extracts used for western-blot analysis obtained from plants grown on MS medium (black bars) or 3 d on MS medium and 5 d on MS medium supplemented with 30 μM MFZ (gray bars). Values in B and D are means ± SD ($n = 3$). Asterisks indicate values that are significantly different (**, $P < 0.005$) compared with those in the EV control plants.

grown with and without MFZ revealed significant reductions in the levels of bulk membrane sterols when amiFPS plants were grown with MFZ. The levels of β-sitosterol in silenced amiFPSa and amiFPSb plants were 36% and 25% lower, respectively, than in MFZ-treated EV plants, whereas those of campesterol decreased by 42% and 30%, respectively (Fig. 3A). A much more prominent reduction was observed in the case of stigmasterol, with decreases of 70% and 66%, respectively (Fig. 3A). Interestingly, these changes also led to a marked reduction of the stigmasterol-to-β-sitosterol ratio, which has a critical role in modulating cell membrane integrity and properties (Schuler et al., 1991; Grosjean et al., 2015) and the normal function of membrane-located proteins (Hartmann, 1998) and is known to influence plant disease resistance and affect the outcome of particular plant-pathogen interactions (Griebel and Zeier, 2010; Wang et al., 2012b). This ratio decreased by 53% and 54.5% in amiFPSa and amiFPSb plants treated with MFZ, respectively, compared with MFZ-treated EV plants (Fig. 3B), while the campesterol-to-β-sitosterol ratio remained unchanged. Quantitative analysis of ubiquinones using ultra-performance liquid chromatography-mass spectrometry showed that the levels of the major ubiquinone species (UQ-9) were decreased by 30% in silenced amiFPSa and amiFPSb plants compared with EV plants grown on medium supplemented with MFZ, whereas the levels of UQ-10, a minor ubiquinone species in Arabidopsis, were increased drastically by 3 and 4 times, respectively (Fig. 3C).

Recent reports have shown that a selective blockage of the sterol pathway triggers a positive feedback regulatory response of HMGR, the main regulatory enzyme of the MVA pathway (Wentzinger et al., 2002; Babiychuk et al., 2008; Nieto et al., 2009; Posé et al., 2009). Such a regulatory response also has been reported in Arabidopsis seeds with reduced levels of FPS activity (Closa et al., 2010; Keim et al., 2012). HMGR activity measurements in amiFPSa, amiFPSb, and EV plants grown with and without MFZ revealed that down-regulation of FPS activity at the early stages of plant development triggers a similar response. Treatment of amiFPSa and amiFPSb plants with MFZ resulted in compensatory up-regulation of HMGR activity of 3.4- and 1.7-fold, respectively, compared with that in MFZ-treated EV plants, which in turn was similar to that in noninduced amiFPS and EV plants (Fig. 4A). Comparison of HMGR activity values (Fig. 4A) with results of protein-blot analysis (Fig. 4B) using polyclonal antibodies raised against the catalytic domain of Arabidopsis HMGR1 (Masferrer et al., 2002) strongly suggested that up-regulation of HMGR activity in FPS-silenced plants occurs at the posttranslational level. This is supported by the observation that HMGR activity in extracts from amiFPSa and amiFPSb plants treated with MFZ was clearly higher than in control plants (Fig. 4A), even though HMGR protein levels in the same extracts were slightly or clearly lower than in the corresponding controls (Fig. 4B). Indeed, expression levels of the two Arabidopsis genes (*HMG1* and *HMG2*) encoding HMGR (Enjuto et al., 1994) were very similar in all the tested lines grown on MS medium supplemented or not with MFZ (Fig. 4C). Altogether, these data indicated that the activation of HMGR in response to silencing of FPS occurs through a posttranslational regulatory mechanism.

The combined effect of FPS down-regulation and the activation of HMGR might lead to the accumulation of cytotoxic levels of pathway intermediaries upstream of

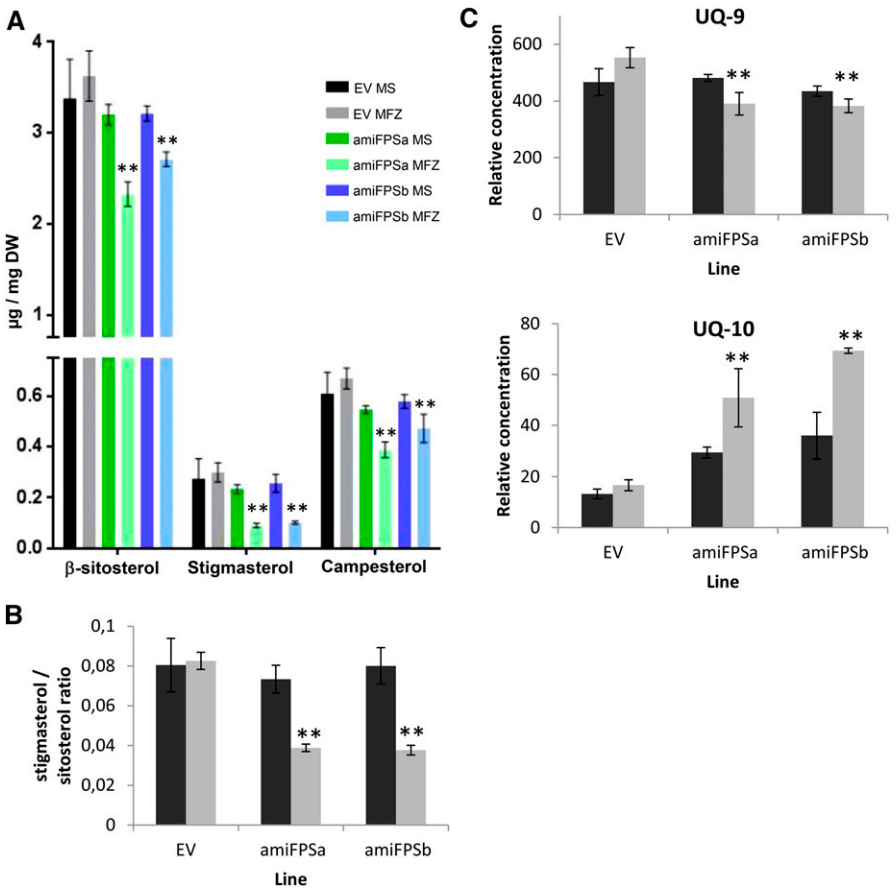

Figure 3. Down-regulation of FPS activity leads to altered profiles of sterols and ubiquinones. Bulk membrane sterols (A), stigmasterol-to-β-sitosterol ratio (B), and ubiquinones UQ-9 and UQ-10 (C) are shown in EV, amiFPSa, and amiFPSb plants grown for 8 d on MS medium (black bars) or 3 d on MS medium and 5 d on MS medium supplemented with 30 μM MFZ (gray bars). Values are means ± SD (n = 3). Asterisks indicate values that are significantly different (**, $P < 0.005$) compared with those in the EV control plants. DW, Dry weight.

FPP (Fig. 1A) that could be responsible for the phenotype of FPS-silenced plants. However, the addition of 5 mM MVA to the growth medium did not enhance the phenotype of these plants (Fig. 4D), indicating that it is caused by the reduced accumulation of an FPP-derived compound. As mentioned above, the down-regulation of FPS leads to an important reduction of campesterol levels (Fig. 3A). This sterol is the biosynthetic precursor of brassinosteroids (Fujioka and Yokota, 2003), which raised the question of whether a deficiency of these hormones could trigger the phenotype of FPS-silenced plants. However, our finding that the addition of 0.4 nM *epi*-brassinolide was unable to rescue the phenotype linked to the down-regulation of FPS (Supplemental Fig. S2) ruled out this possibility.

Down-Regulation of FPS Alters Chloroplast Development and Plastidial Isoprenoid Levels

The chlorotic phenotype displayed by FPS-silenced plants strongly suggested that chloroplast structure and function might be affected in these plants. Confocal laser microscopy analysis of leaves revealed a strong reduction in the chloroplast area of amiFPSa- and amiFPSb-silenced plants compared with EV plants grown under the same conditions (i.e. about 55% and 38% of control chloroplast area, respectively; Fig. 5, A and C). A closeup inspection of the confocal microscopy images also showed that chloroplasts of FPS-silenced plants contained darker regions likely devoid of chlorophyll (Fig. 5A), suggesting that chloroplast ultrastructure also was affected. Indeed, chloroplasts of amiFPSa and amiFPSb plants treated with MFZ showed severe morphological alterations, including an irregular outer membrane envelope, disorganized and less abundant thylakoid membranes, massive accumulations of starch granules, and a large number of electron-dense particles that are likely to correspond to plastoglobuli. On the contrary, chloroplasts of EV plants treated with MFZ showed normal structure, with well-organized thylakoid membranes and a regular shape (Fig. 5B), and looked indistinguishable from chloroplasts of amiFPSa, amiFPSb, and EV plants grown on MS medium. Altogether, these data indicated that normal levels of FPS activity are essential for proper chloroplast development.

When the photosynthesis-related isoprenoid metabolites were quantified in all these plants, a drastic reduction of chlorophyll (*a* and *b*) and carotenoid levels (50%–60%) was observed in MFZ-treated amiFPS plants compared with EV plants grown under the same conditions (Fig. 5D). A more detailed analysis of the carotenoid fraction confirmed a sharp decline in β-carotene, lutein, and violaxanthin-neoxanthin

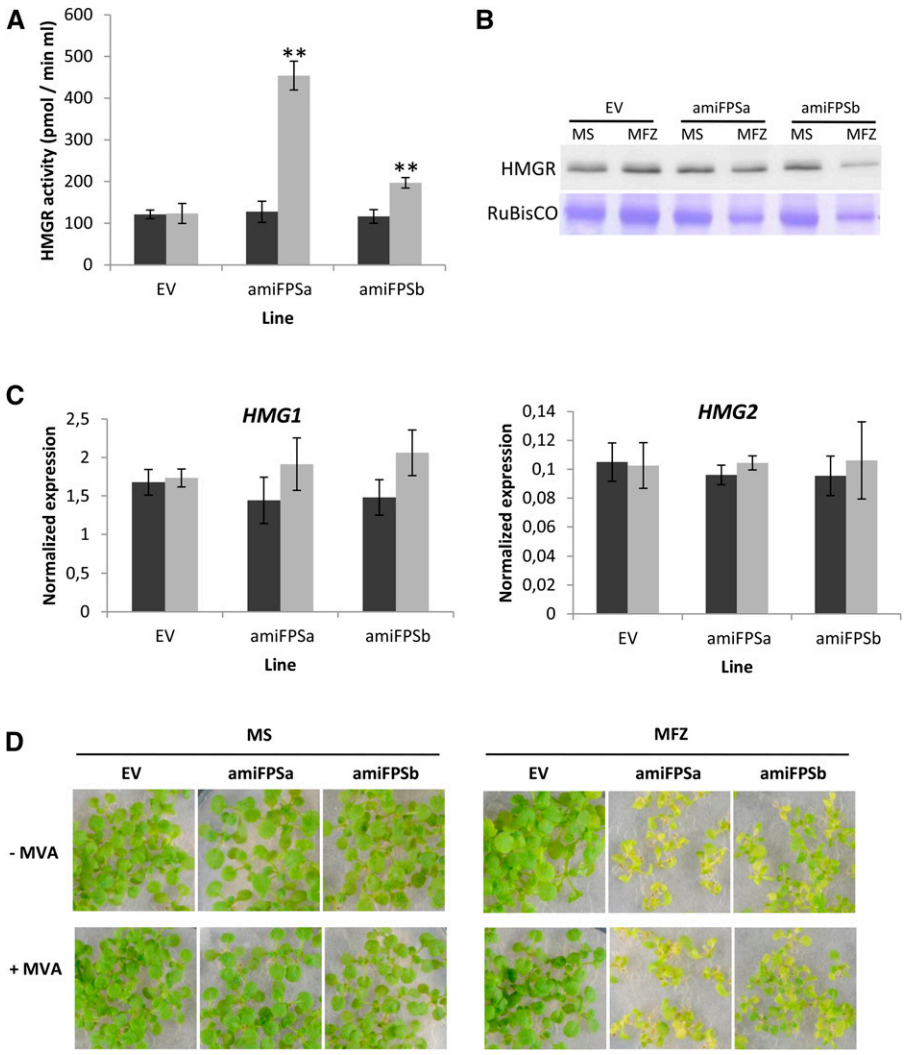

Figure 4. Down-regulation of FPS activity triggers the posttranslational up-regulation of HMGR activity. A, HMGR activity measured in extracts from EV, amiFPSa, and amiFPSb plants grown for 8 d on MS medium (black bars) or 3 d on MS medium and 5 d on MS medium supplemented with 30 μM MFZ (gray bars). Values are means ± SD (n = 3). Asterisks indicate values that are significantly different (**, $P < 0.005$) compared with those in the EV control plants. B, Western-blot analysis of HMGR protein (top) and Coomassie Brilliant Blue-stained large subunit of Rubisco (bottom) in the same extracts used for HMGR activity determination. Membranes show the results of a representative experiment. C, RT-qPCR analysis of *HMG1* and *HMG2* mRNA levels using RNA from EV, amiFPSa, and amiFPSb seedlings grown on MS medium (black bars) or 3 d on MS medium and 5 d on MS medium supplemented with 30 μM MFZ (gray bars). Transcript levels were normalized relative to the mRNA levels of the *PP2AA3* gene. Values are means ± SD (n = 3). D, Phenotypes of 8-d-old EV, amiFPSa, and amiFPSb seedlings grown with or without 5 mM MVA on MS medium (left) or 3 d on MS medium and 5 d on MS medium supplemented with 30 μM MFZ (right).

contents in MFZ-treated amiFPS plants compared with EV plants grown on medium with MFZ. The levels of these metabolites decreased, respectively, by 57%, 48%, and 53% in amiFPSa plants and by 45%, 36%, and 35% in amiFPSb plants (Supplemental Fig. S3A). The levels of other important plastidial isoprenoid compounds, such as prenylquinones, also were strongly altered. The levels of phylloquinone and plastochromanol-8 were markedly reduced in silenced amiFPS plants (42% in amiFPSa plants and 23% and 29%, respectively, in amiFPSb plants), while those of plastoquinone-9 were only slightly reduced (16% only in amiFPSa plants; Supplemental Fig. S3B). On the contrary, the levels of tocopherols (phytyl-derived side chain compounds) were increased, as in the case of γ-tocopherol (3.2- and 2.4-fold in amiFPSa and amiFPSb plants, respectively), or remained unchanged, as observed for α- and δ-tocopherols (Supplemental Fig. S3C). Altogether, these results demonstrated that down-regulation of FPS activity has a strong negative impact on plastidial isoprenoid metabolism in addition to the detrimental effect on cytosol/ER isoprenoid biosynthesis.

Transcriptional Profiling of Plants Silenced for FPS Reveals Misregulation of Genes Involved in the JA Pathway, Abiotic Stress Response, Fe and Redox Homeostasis, and Carbohydrate Metabolism

To get insight into the molecular phenotypes of Arabidopsis plants with reduced levels of FPS activity, global changes of gene expression in FPS-silenced plants relative to nonsilenced plants were investigated using an RNA sequencing (RNA-seq)-based approach. Using RNA samples from three independent biological replicates of amiFPSa plants grown on MS medium supplemented or not with MFZ, two complementary DNA (cDNA) libraries were constructed and sequenced with an Illumina HiSeq 2000 platform. After trimming the obtained raw reads to remove adaptor sequences, empty reads, and low-quality sequences, a total of 168,617,824 and 144,342,444 high-quality reads, designated as clean reads, were generated for amiFPSa plants grown on MS medium supplemented or not with MFZ, respectively, of which 99.29% and 98.18% were paired-end reads and 0.71% and 1.82% were single-end

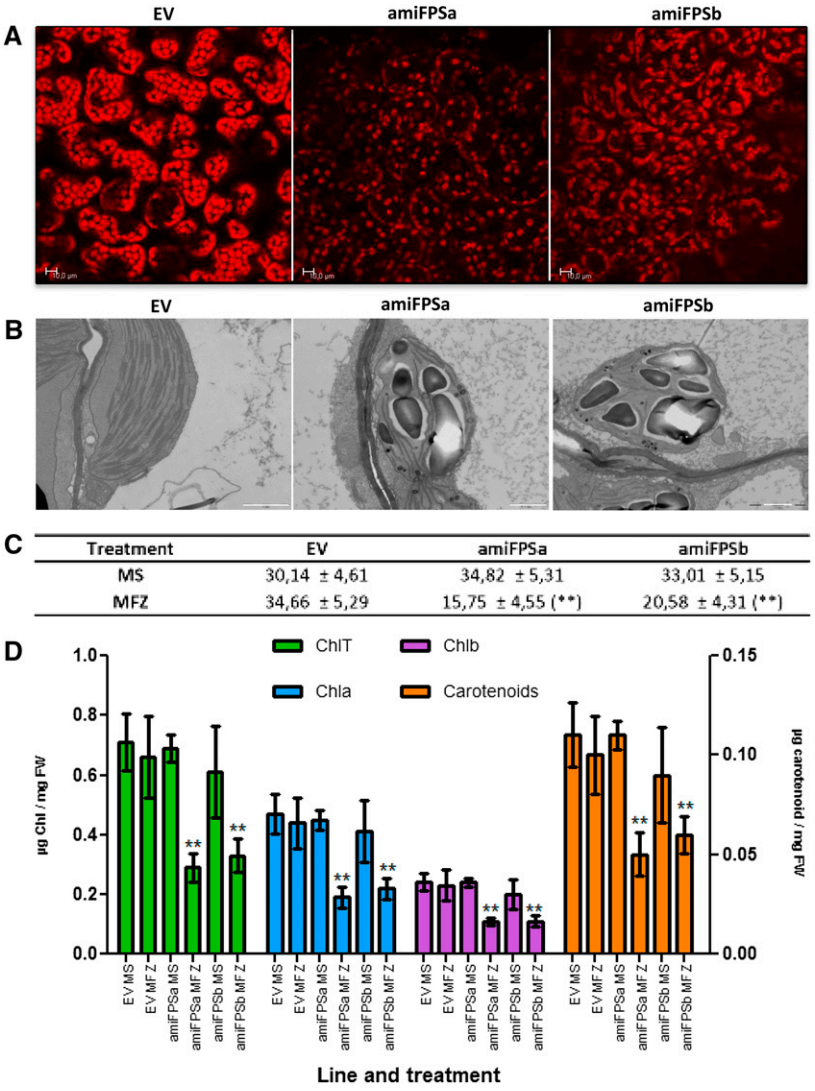

Figure 5. Down-regulation of FPS activity alters chloroplast development as well as chlorophyll and carotenoid levels. A to C, Laser confocal microscopy (A), transmission electron microscopy (B), and area (μm^2) of chloroplasts (C) in leaves is shown for plants grown for 3 d on MS medium and 5 d on MS medium supplemented with 30 μM MFZ. Chloroplast area values are expressed as means ± SD ($n = 36$). Bars = 10 μm (A) and 1 μm (B). D, Chlorophyll (total, chlorophyll *a*, and chlorophyll *b*) and carotenoid contents in EV, amiFPSa, and amiFPSb plants grown for 8 d on MS medium or 3 d on MS medium and 5 d on MS medium supplemented with 30 μM MFZ. Values are means ± SD ($n = 3$). Asterisks indicate values that are significantly different (**, $P < 0.005$) compared with those in the EV control plants. FW, Fresh weight.

reads. Almost all clean reads (97% and 98%, respectively) were successfully mapped to The Arabidopsis Information Resource (TAIR) 10 version of the Arabidopsis reference genome. Fragments per kilobase of exon per million fragments mapped-normalized read counts were obtained from each of the samples and employed for differential gene expression analysis. The resulting list of differentially expressed genes was filtered by $\log_2$ (fold change) of 2 or greater or −2 or less and a statistical value of $q = 0.05$. On this basis, a total of 168 differentially expressed genes were identified in FPS-silenced plants compared with nonsilenced plants, including 116 up-regulated genes and 16 down-regulated genes. Additionally, we found 35 genes that were expressed only in FPS-silenced plants (switch-on genes) and a single gene that was expressed only in nonsilenced plants (switch-off gene; Supplemental Table S1). Classification of differentially expressed genes using Gene Ontology biological process functional domains revealed an overrepresentation of genes involved in stress responses. The biotic stress response, including the response to bacterial and fungal infections, signal transduction, regulation of systemic acquired resistance, and response to salicylic acid (SA) stimulus (Fig. 6), was the most represented one. Remarkably, 15 genes were assigned to the category of JA response, including genes involved in JA biosynthesis, signaling, and homeostasis. Adding to this category six other genes reported to be specific targets of the JA response brought the total number of up-regulated JA-related genes to 19 (Table I), or 11.5% of the total differentially expressed genes (Supplemental Table S1). In the abiotic stress category, the main responses were related to wounding, salt, cold, and water deprivation (Fig. 6), and genes included in this category were both up- and down-regulated (Table I). Genes encoding proteins related to Fe homeostasis and redox functions also were prominent among the misregulated genes (Table I). Interestingly, those associated with Fe storage, metabolism, and transport were down-regulated, whereas those coding for proteins involved in sensing and signaling of Fe deficiency were up-regulated. In the

group of misregulated redox genes, all but one were up-regulated. Finally, we also identified a group of misregulated genes coding for proteins related to carbohydrate metabolism (Table I), a transcriptional response consistent with the altered chloroplast development observed in the FPS-silenced plants.

Inhibition of Sterol Biosynthesis Mimics the Transcriptional Response to Down-Regulation of FPS

As mentioned previously, the phenotypic alterations displayed by FPS-silenced plants are not due to the accumulation of MVA or a derived compound upstream of FPP (Fig. 4D) but, rather, to the reduced levels of an FPP-derived compound other than brassinosteroids (Supplemental Fig. S2). This, together with the marked reduction of bulk membrane sterols detected in these plants (Fig. 3, A and B) and the suggested possible connection between impaired sterol biosynthesis and altered chloroplast development (Babiychuk et al., 2008; Kim et al., 2010), prompted us to investigate whether sterol depletion is responsible for the transcriptional response to FPS silencing. To this end, we compared the mRNA levels of 39 genes representative of the main physiological responses observed in FPS-silenced plants (Table I) with those in wild-type plants treated with terbinafine (Tb), a specific inhibitor of squalene epoxidase (SQE; Ryder, 1992), and *cvp1/smt3* mutant plants (Carland et al., 2010). SQE catalyzes the synthesis of 2,3-oxidosqualene from squalene, the first committed precursor of sterols. SMT2 and SMT3 are both sterol-C24-methyltransferases responsible for the methylation of 24-methylene lophenol to produce 24-ethylidene lophenol, the reaction that distinguishes the synthesis of the structural sterols β-sitosterol and stigmasterol from campesterol and the signaling brassinosteroid derivatives (Schaller, 2003; Carland et al., 2010; Fig. 7A). Thus, we performed a real-time reverse transcription-quantitative PCR (RT-qPCR) expression analysis for genes included in the categories of JA pathway (*LOX4*, *AOC1*, *AOC3*, *CLO-3*, *CYP94B3*, *ST2A*, *JAZ1*, *JAZ5*, *WRKY33*, *JAL23*, *ABCG40*, *VSP1*, *JR2*, and *ATCLH1*), abiotic stress (*AKR4C8*, *AKR4C9*, *COR78*, *COR414*, *COR15B*, and *RAP2.6L*), Fe homeostasis (*NEET*, *FER1*, *FER4*, *MLP329*, *BHLH038*, *BHLH039*, and *BHLH100*), redox homeostasis (*GST22*, *GSTF6*, *GSTF12*, *Prx37*, and *WCRKC1*), carbohydrate metabolism (*DIN11*, *BMY1*, *SCORP*, *GPT2*, and *FBA5*), and two genes not included in the above categories (*ILL6* and *MLP328*), using RNA from amiFPSa and EV plants treated with MFZ, wild-type plants treated or not with 150 μM Tb, and *cvp1/smt3* mutant plants grown on MS medium. The fold change in the expression levels of the selected genes for each treatment were calculated relative to their corresponding controls, and the results are represented as a heat map (Fig. 7B). Overall, the comparison of the RT-qPCR and RNA-seq expression results in FPS-silenced plants showed that all tested genes were misregulated in the same way (10 genes repressed and 29 genes induced), thus confirming the differential gene expression analysis results obtained in the RNA-seq analysis (Table I; Supplemental Table S1). Additionally, there was a very high degree of qualitative correlation between gene expression changes in plants silenced for FPS and plants where the sterol pathway was inhibited chemically (Tb) or genetically (*cvp1/smt3* mutant). In both cases, 35 genes (i.e. 90% of the analyzed genes) were misregulated in the same way when compared with FPS-silenced plants, while only four genes were misregulated in the opposite direction. Three of the latter (*COR78*, *COR414*, and *COR15B*), unlike what happens

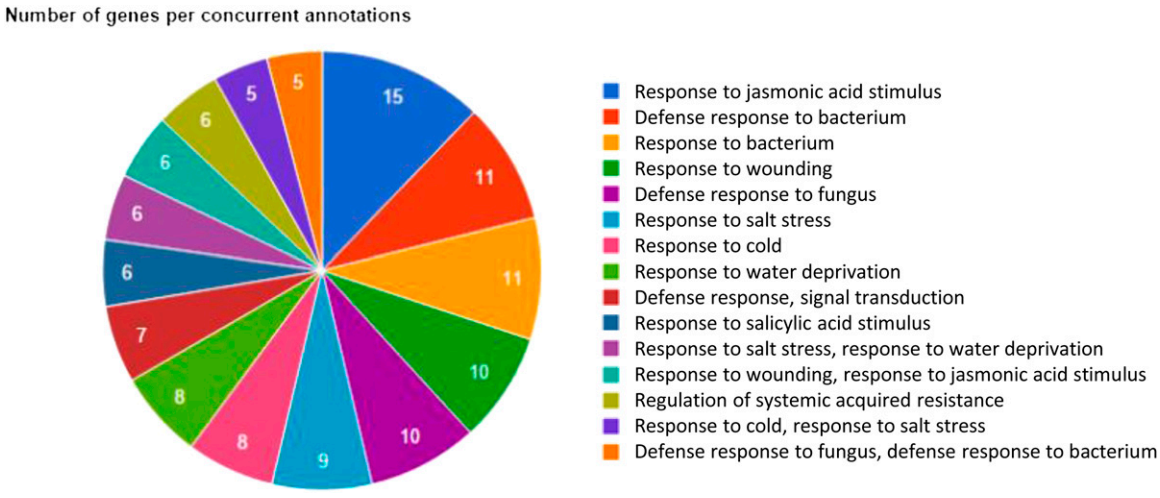

Figure 6. Gene Ontology classification of the differentially expressed genes in FPS-silenced plants. The 168 genes showing at least a $\log_2$ (fold change) of 2 or greater or -2 or less and a q value less than 0.05 (Supplemental Table S1) were classified by the biological process category using the GeneCodis tool (http://genecodis.cnb.csic.es/; Carmona-Saez et al., 2007).

Table I. *Selection of genes that are differentially expressed between amiFPSa plants grown for 8 d on MS medium or 3 d on MS medium and 5 d on MS medium supplemented with 30 μM MFZ*

Gene Name	Gene Symbol	Log_2 Fold Change	*P* Value	*q* Value	Gene Description
Jasmonate synthesis					
AT2G26560	PLA-IIA	3.9	5.00E-05	0.011	Phospholipase A 2A
AT1G72520	LOX4	3.4	0.00035	0.047	PLAT/LH2 domain-containing lipoxygenase family protein
AT3G25760	AOC1	2.9	5.00E-05	0.011	Allene oxide cyclase1
AT3G25780	AOC3	2.8	5.00E-05	0.011	Allene oxide cyclase3
Jasmonate homeostasis					
AT3G48520	CYP94B3	4.7	0.0003	0.042	Cytochrome P450, family 94, subfamily B, polypeptide 3
AT5G07010	ST2A	2.9	0.0003	0.042	Sulfotransferase2A
Jasmonate signaling					
AT1G17380	JAZ5	4.5	0.0002	0.032	Jasmonate-zim-domain protein5
AT1G19180	JAZ1	3.6	5.00E-05	0.011	Jasmonate-zim-domain protein1
AT5G13220	TIFY9	3.6	5.00E-05	0.011	Jasmonate-zim-domain protein10
AT1G70700	JAZ9	2.6	5.00E-05	0.011	TIFY domain/divergent CCT motif family protein
AT1G72450	JAZ6	2.3	0.0001	0.019	Jasmonate-zim-domain protein6
AT3G56400	WRKY70	4.1	5.00E-05	0.011	WRKY DNA-binding protein70
AT2G38470	WRKY33	2.2	0.00015	0.025	WRKY DNA-binding protein33
Jasmonate targets					
AT2G39330	JAL23	6.7	5.00E-05	0.011	Jacalin-related lectin23
AT1G15520	ABCG40	6.2	5.00E-05	0.011	Pleiotropic drug resistance12
AT5G24780	VSP1	5.4	5.00E-05	0.011	Vegetative storage protein1
AT2G34810	AT2G34810	3.8	5.00E-05	0.011	FAD-binding berberine family protein
AT4G23600	JR2	3.7	5.00E-05	0.011	Tyr transaminase family protein
AT1G19670	ATCLH1	2.8	5.00E-05	0.011	Chlorophyllase1
Abiotic stress					
AT5G13330	Rap2.6L	3.8	0.0001	0.019	Related to AP2 6l
AT2G37770	AKR4C9	3.7	5.00E-05	0.011	NAD(P)-linked oxidoreductase superfamily protein
AT2G33380	CLO-3	3	5.00E-05	0.011	Caleosin-related family protein
AT4G02330	ATPMEPCRB	2.5	5.00E-05	0.011	Plant invertase/pectin methylesterase inhibitor superfamily
AT2G37760	AKR4C8	2.2	0.00015	0.025	NAD(P)-linked oxidoreductase superfamily protein
AT5G52310	COR78	−2.4	0.00035	0.047	Cold regulated78
AT1G29395	COR414-TM1	−3.1	5.00E-05	0.011	Cold regulated314 thylakoid membrane 1
AT2G42530	COR15B	−3	5.00E-05	0.011	Cold regulated15b
Fe homeostasis					
AT3G56970	BHLH038	4	5.00E-05	0.011	Basic helix-loop-helix DNA-binding superfamily protein
AT2G41240	BHLH100	3.8	5.00E-05	0.011	Basic helix-loop-helix protein100
AT3G56980	BHLH039	3.5	0.0001	0.019	Basic helix-loop-helix DNA-binding superfamily protein
AT2G01530	MLP329	−2.4	5.00E-05	0.011	MLP-like protein329
AT2G40300	FER4	−2.4	0.0001	0.019	Ferritin4
AT3G25190	VTL5	−2.4	0.0001	0.019	Vacuolar Fe transporter family protein
AT5G01600	FER1	−2.6	0.00025	0.037	Ferretin1
AT5G51720	NEET	−4	5.00E-05	0.011	Two Fe, two sulfur cluster binding
Redox homeostasis					
AT1G69880	ATH8	4.5	0.0002	0.032	No description available
AT2G29460	GST22	4.2	0.00035	0.047	GST τ4
AT1G02930	ATGSTF6	3.7	5.00E-05	0.011	GST6
AT1G02920	GST11	3	5.00E-05	0.011	GST7
AT4G08770	Prx37	2.8	0.0001	0.019	Peroxidase superfamily protein
AT5G17220	ATGSTF12	2.7	0.0001	0.019	GST ϕ12
AT3G49110	ATPCA	2.2	0.00025	0.037	Peroxidase CA
AT5G06690	WCRKC1	−2.3	0.0001	0.019	WCRKC thioredoxin1
Carbohydrate metabolism					
AT3G49620	DIN11	5.6	5.00E-05	0.011	2-Oxoglutarate and Fe(II)-dependent oxygenase superfamily protein
AT3G60140	DIN2	5.2	5.00E-05	0.011	Glycosyl hydrolase superfamily protein
AT4G15210	BMY1	4.2	0.00025	0.037	β-Amylase5
AT2G43530	SCORP	3.2	5.00E-05	0.011	Scorpion toxin-like knottin superfamily protein
AT1G61800	GPT2	3.1	5.00E-05	0.011	Glc-6-P/phosphate translocator2

(*Table continues on following page.*)

Table I. (*Continued from previous page.*)

Gene Name	Gene Symbol	Log_2 Fold Change	*P* Value	*q* Value	Gene Description
AT5G24420	PGL5	2.5	0.0001	0.019	6-Phosphogluconolactonase5 OPP shunt
AT4G26530	FBA5	−3.1	0.0001	0.019	Aldolase superfamily protein
Others					
AT1G44350	ILL6	2.8	0.0001	0.019	IAA-Leu resistant-like gene6
AT2G01520	MLP328	−2.4	0.00015	0.025	MLP-like protein328

in FPS-silenced plants, were induced upon specific inhibition of the sterol pathway and belong to the same group of cold-responsive genes (Table I). The fourth differentially expressed gene was *WRCKC1* in plants treated with Tb and *AOC3* in the *cvp1/smt3* plants. In fact, these are the only two differentially regulated genes between plants treated with Tb and the *cvp1/smt3* plants, which means that 95% of the genes tested in these plants were misregulated in the same way. Altogether, these data indicated that inhibition of sterol biosynthesis triggers a transcriptional response highly similar to that observed in plants with a compromised synthesis of FPP, suggesting that depletion of sterols is the primary cause of the molecular and physiological phenotypes observed in FPS-silenced plants.

Time-Course Expression Analysis Reveals an Early Response of Misregulated Genes after FPS Silencing

To determine if the transcriptional responses observed in FPS-silenced plants were a primary effect or a secondary consequence of FPS down-regulation, we conducted a time-course expression analysis of a subset of genes representative of the different functional categories shown in Table I. To this end, amiFPSa and EV plants were grown on MS medium for 3 d, transferred to MS medium supplemented with MFZ, and sampled at different time points (0, 4, 8, 12, and 24 h) for RNA extraction. The JA-related transcriptional response was analyzed by quantifying the transcript levels of representative genes involved in JA biosynthesis (*LOX4*), signaling (*JAZ1* and *JAZ5*), and homeostasis (*ST2A*) as well as JA target genes (*JR2*, *VSP1*, and *ABCG40/PDR12*; Campbell et al., 2003; Wasternack and Hause, 2013). As shown in Figure 8A, the mRNA levels of *LOX4*, *JAZ1*, and *JAZ5* started to increase almost immediately after the induction of silencing, suggesting that down-regulation of FPS triggers an early activation of JA biosynthesis and signaling pathways. This was further supported by the progressive increase of mRNA levels observed for the JA-responsive defense genes *JR2*, *ABCG40/PDR12*, and *VSP1* after the induction of FPS silencing, which reached a maximum at the end of the time course. Interestingly, mRNA levels of *ST2A*, a gene involved in JA homeostasis, were early down-regulated, suggesting a concomitant reduction of the JA catabolic turnover, which in the long term appears to be activated because, 5 d after the induction of silencing, *ST2A* mRNA levels were clearly higher in the FPS-silenced plants than in the nonsilenced ones (Table I; Fig. 7B). The expression of three representative genes (*AKR4C8*, *AKR4C9*, and *COR78*) known to be misregulated in response to different abiotic stresses, including drought, heat, cold, salt, and osmotic stress, also was analyzed. *AKR4C8* and *AKR4C9* encode two members of the aldo-reductase family involved in the detoxification of stress-induced reactive carbonyls (Sengupta et al., 2015), and *COR78* is a gene reported as responsive to cold (Nordin et al., 1991; Horvath et al., 1993). As shown in Figure 8B, in FPS-silenced plants, *AKR4C8* and *AKR4C9* mRNA levels were strongly increased from the very beginning and throughout the entire time course analysis compared with nonsilenced plants. On the contrary, *COR78* mRNA levels were consistently lower throughout the entire time course, with the only exception of time point 12 h. Overall, these results confirmed the close relationship between defective sterol biosynthesis and the induction of the JA pathway and demonstrated that plants quickly perceive a disruption of sterol homeostasis as a stress signal that triggers an early misregulation of stress-related genes.

The Fe deficiency transcriptional response to FPS silencing was investigated by measuring the mRNA levels of genes coding for proteins involved in Fe plastid storage (*FER1* and *FER4*; Briat et al., 2010) and metabolism (*NEET*; Nechushtai et al., 2012) as well as proteins involved in sensing and signaling of Fe deficiency (*bHLH038*, *bHLH039*, and *bHLH100*; Rodríguez-Celma et al., 2013; Fig. 9A). *FER4* transcripts were markedly down-regulated throughout the time-course analysis, whereas *FER1* mRNA levels showed a similar but milder initial depletion followed by a significant increase above the levels detected in control plants after 24 h of FPS silencing. However, in the long term, the *FER1* transcript levels were again lower than in control plants (Table I; Fig. 7B). The *NEET* transcript levels also decreased over the entire time course, albeit to a different extent depending on the time point. The impact of FPS silencing on Fe homeostasis was further confirmed by quantifying the mRNA levels of three members of the Ib subgroup of bHLH transcription factors that are induced by Fe deficiency. *bHLH038*, *bHLH39*, and *bHLH100* mRNA levels changed in a very similar way, with increases over the first 8 h after FPS silencing followed by reductions at time points 12 and 24 h (Fig. 9A). After 5 d of silencing, the mRNA levels of these genes in FPS-silenced plants were again higher

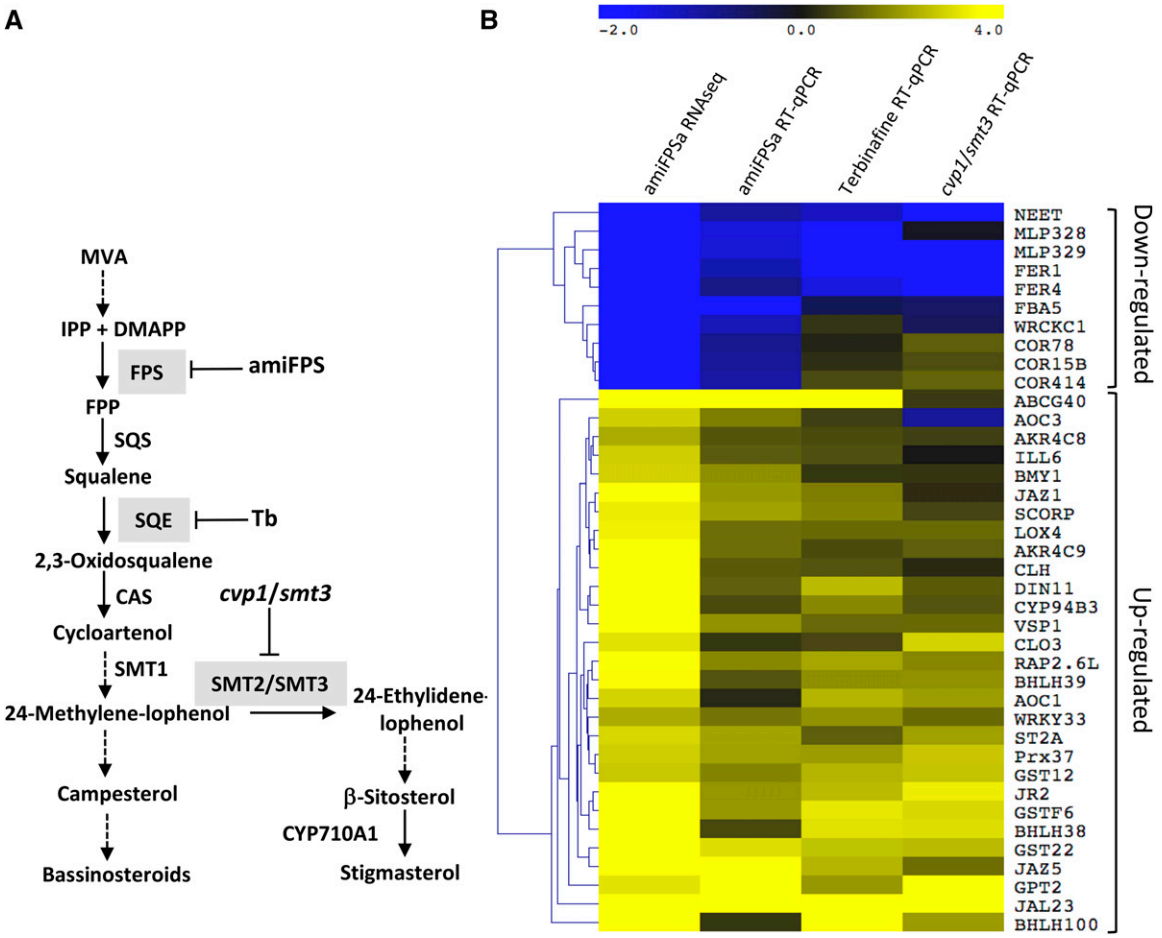

Figure 7. Inhibition of the sterol biosynthetic pathway mimics the transcriptional response of FPS-silenced plants. A, Simplified scheme of the post-MVA sterol biosynthesis pathway. The positions of reactions catalyzed by FPS, squalene synthase (SQS), squalene epoxidase (SQE), cycloartenol synthase (CAS), sterol methyltransferases (SMT1, SMT2, and SMT3), and sterol C22 desaturase (CYP710A1) are shown. Dashed arrows represent multiple enzymatic steps. B, Heat map showing the expression changes of a selection of 39 representative genes (Table I) in seedlings silenced for FPS (amiFPSa) and seedlings where the sterol pathway was inhibited chemically with 150 μM Tb or genetically (*cvp1/smt3*). The color scale indicates the level of gene expression change, with values ranging from $\log_2$ fold change −2 (lower expression, blue color) to 4 (higher expression, yellow color). Hierarchical clustering was done using the Euclidean distance. Rows represent genes, and columns represent the fold change of mRNA levels for each gene under each experimental condition compared with its corresponding control: amiFPSa RNAseq, amiFPSa seedlings grown for 3 d on MS medium and 5 d on MS medium supplemented with 30 μM MFZ versus amiFPSa seedlings grown for 8 d on MS medium; amiFPSa RT-qPCR, amiFPSa versus EV seedlings both grown for 3 d on MS medium and 5 d on MS medium supplemented with 30 μM MFZ; Tb RT-qPCR, Col-0 seedlings grown for 8 d on MS medium supplemented with 150 μM Tb versus Col-0 seedlings grown on MS medium; *cvp1/smt3* RT-qPCR, *cvp1/smt3* seedlings versus Col-0 seedlings grown for 8 d on MS medium.

than in control plants (Table I; Fig. 7B). Overall, the long-term Fe-related gene expression changes pointed to a Fe deficiency, which was confirmed by the finding that Fe levels in MFZ-treated amiFPS plants were 30% lower than in EV plants grown on MFZ (Fig. 9B). Moreover, the rapid and highly coordinated response of all these Fe-related genes strongly suggests that the perturbation of Fe cellular homeostasis (Fig. 9B) is an early consequence of FPS silencing and sterol depletion.

To analyze the time course of the oxidative stress-related transcriptional response, we investigated the expression of genes coding for the glutathione *S*-transferases GST6, GST12, and GST22 (Dixon et al., 2010; Foyer and Noctor, 2011) and the peroxidase Prx37 (Shin et al., 2005). Interestingly, the mRNA levels of these genes showed the same qualitative pattern of changes throughout the time-course analysis (Supplemental Fig. S4A). Silencing of FPS led to decreased mRNA levels of all four genes from the very beginning throughout the entire time course, *GST6* and *GST12* being the most deeply repressed, with the one exception of time point 12 h. The early down-regulation of these antioxidant genes is in sharp contrast to their long-term response, since 5 d after the induction of

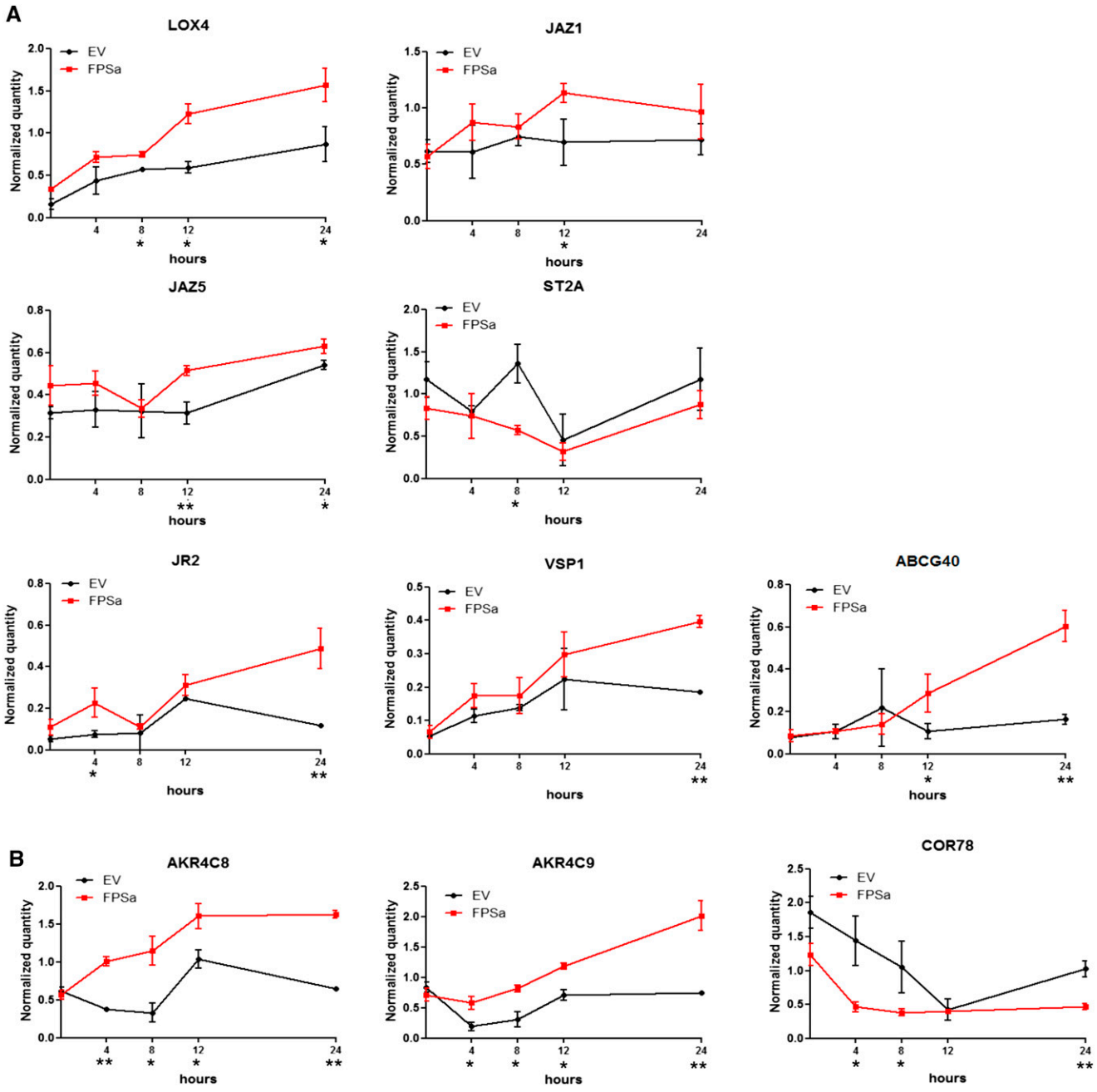

Figure 8. Plants perceive a reduction in bulk membrane sterols as a stress signal that triggers an early up-regulation of genes involved in both biotic and abiotic stress responses. Three-day-old amiFPSa and EV seedlings grown on MS medium were transferred to MS medium supplemented with 30 μM MFZ, and tissue samples were collected at the indicated time points from the start of MFZ treatment. The mRNA levels of genes involved in the JA pathway (A), including JA synthesis (*LOX4*), signaling (*JAZ1* and *JAZ5*), homeostasis (*ST2A*), and target genes (*JR2*, *VSP1*, and *ABCG40*), and different abiotic stress responses (B; *AKR4C8*, *AKR4C9*, and *COR78*) were quantified by RT-qPCR using RNA samples from seedlings collected at the indicated time points. Data are expressed as means of normalized quantity values ± SD ($n = 3$) calculated using three independent housekeeping genes (*UBC*, *UBC9*, and *PP2A*; Ballester et al., 2013). Asterisks indicate values that are significantly different (*, $P < 0.05$ and **, $P < 0.005$) compared with those in the EV control plants.

silencing, the mRNA levels of all four genes were much higher than in nonsilenced plants (Table I; Fig. 7B). This antioxidant response might account for the absence of oxidative stress symptoms in the leaves of FPS-silenced plants compared with control plants (Supplemental Fig. S4B). Either way, the results are indicative of an early disturbance of cellular redox homeostasis in response to FPS silencing.

Lastly, we investigated the expression of selected genes coding for proteins related to carbohydrate

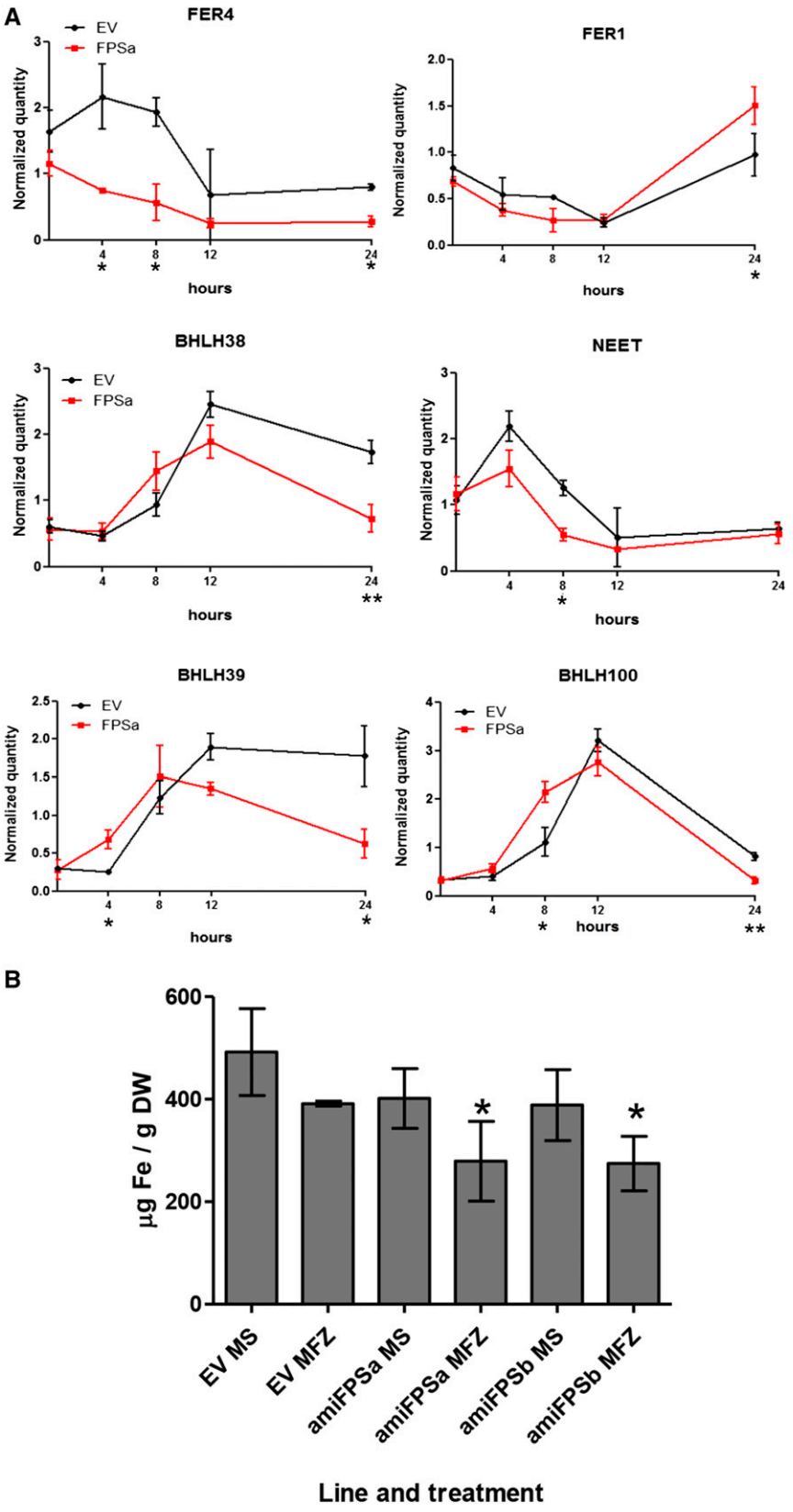

Figure 9. Down-regulation of FPS causes the early misregulation of genes involved in maintaining Fe homeostasis. A, The mRNA levels of genes encoding proteins involved in Fe storage (*FER1* and *FER4*), metabolism (*NEET*), and sensing and signaling (*BHLH038*, *BHLH039*, and *BHLH100*) were quantified by RT-qPCR using RNA samples from seedlings collected at the indicated time points. Data are expressed as means of normalized quantity values ± SD ($n = 3$) calculated using three independent housekeeping genes (*UBC*, *UBC9*, and *PP2A*; Ballester et al., 2013). Asterisks indicate values that are significantly different (*, $P < 0.05$ and **, $P < 0.005$) compared with those in the EV control plants. B, Fe levels in samples of EV, amiFPSa, and amiFPSb seedlings grown for 8 d on MS medium or 3 d on MS medium and 5 d on MS medium supplemented with 30 μM MFZ were determined using an inductively coupled plasma optical emission spectrometer. Values are means ± SD ($n = 3$). Asterisks indicate values that are significantly different (*, $P < 0.05$) compared with the EV control plants. DW, Dry weight.

metabolism, including a defensin-like protein predicted to be involved in maltose and starch metabolism (*SCORP*), an aldolase superfamily protein involved in the Suc signaling pathway (*FBA5*; Lu et al., 2012), a Glc-6-P/phosphate translocator that imports Glc-6-P from cytosol to chloroplast and is induced in response to impaired carbon metabolism or its regulation (*GPT2*; Dyson et al., 2015), a 2-oxoacid-dependent dioxygenase repressed by sugar (*DIN11*; Fujiki et al., 2000, 2001), and β-amylase5 (*BMY1*), the major form of β-amylase in Arabidopsis (Laby et al., 2001). The results showed that FPS silencing triggered an early down-regulation of *SCORP*, *FBA5*, and *GPT2* mRNA levels and a mild but steady up-regulation of *DIN11* mRNA content but had no effect on BMY1 mRNA content over the first 24 h (Supplemental Fig. S5). Interestingly, changes in the mRNA levels of all five genes were much more pronounced at the end of the time course, with strong up-regulation of *BMY1*, *DIN11*, *GPT2*, and *SCORP* mRNA levels and a marked depletion of *FBA5* mRNA (Table I; Fig. 7B). Altogether, these results suggest that carbohydrate metabolism also is altered by the down-regulation of FPS.

DISCUSSION

Down-Regulation of FPS Activity in Arabidopsis amiRNA-Based Conditional Knockdown Mutants

Arabidopsis *fps1* and *fps2* single knockout mutants are viable and almost indistinguishable from wild-type plants, while *fps1/fps2* double knockout mutants are embryo lethal (Closa et al., 2010). This makes it impossible to investigate the biological function of FPS at postembryonic stages using *fps* knockout mutants. To overcome this limitation, we obtained and characterized Arabidopsis mutant lines expressing amiRNAs targeting both Arabidopsis *FPS* genes simultaneously (Fig. 1B) under the control of an ecdysone-inducible expression promoter system (Padidam et al., 2003; Dietrich et al., 2008). When the expression of the amiFPS-coding transgenes was induced after seed germination, amiFPS plants were able to develop the first pair of true leaves, which showed only a slight reduction in size compared with control plants, and displayed a chlorotic phenotype (Fig. 2A). Molecular and biochemical analyses in amiFPS seedlings grown under these conditions showed a strong down-regulation of FPS1 and FPS2 transcripts that resulted in a pronounced reduction of total FPS protein and enzyme activity levels (Fig. 2). The finding that the expression of both amiRNAs caused the same phenotype, together with the fact that it was fully complemented by the constitutive expression of isoform FPS1S (Masferrer et al., 2002; Supplemental Fig. S1), confirmed that the phenotype was specifically due to the down-regulation of FPS and not to undesired side effects caused by the misregulation of unpredicted off targets and/or artifacts derived from the inducible silencing system used. It is worth noting that full reversion of the phenotype was achieved even though FPS mRNA levels in the double transgenic plants amiFPSa/35S::FPS1 were not fully restored to wild-type levels (Supplemental Fig. S1C), which is in agreement with the notion that wild-type levels of FPS activity are not limiting in the isoprenoid pathway (Manzano et al., 2004). Interestingly, FPS2 mRNA levels in the double transgenic plants also were higher than in amiFPSa plants (Supplemental Fig. S1C), most likely because large amounts of amiFPSa (Supplemental Fig. S1D) are diverted to silence both endogenous and ectopic *FPS1* gene expression at the expense of the amount of amiFPSa available for the silencing of *FPS2* expression.

Previous studies have shown that both the genetic and pharmacological block of the sterol biosynthesis pathway leads to a compensatory up-regulation of HMGR activity (Wentzinger et al., 2002; Babiychuk et al., 2008; Nieto et al., 2009; Posé et al., 2009; Closa et al., 2010). In agreement with these observations, HMGR activity also was enhanced in FPS-silenced plants (Fig. 4A), although neither the amount of HMGR protein nor the levels of *HMG1* and *HMG2* transcripts (Fig. 4, B and C) were increased simultaneously, indicating that the mechanism behind HMGR up-regulation is posttranslational. This is fully consistent with the hypothesis that variations of HMGR activity in response to changes in the flux of the MVA-derived isoprenoid pathway occur mainly via post-translational control (Nieto et al., 2009), although the precise nature of this regulatory mechanism remains to be established. HMGR activity levels in FPS-silenced plants may be up-regulated through changes in the phosphorylation status of the enzyme (Dale et al., 1995; Douglas et al., 1997; Leivar et al., 2011) and/or protein degradation mechanisms involving the ERAD protein quality control system (Doblas et al., 2013; Pollier et al., 2013). In any case, an enhancement of HMGR activity concomitant to a reduction of FPS activity could lead to the accumulation of MVA pathway intermediates upstream of FPP that might cause the observed phenotype. For example, MVA at high concentrations has a mild inhibitory effect on the growth of cultured tobacco (*Nicotiana tabacum*) BY-2 cells (Crowell and Salaz, 1992), and the accumulation of high levels of IPP and DMAPP appear to have a cytotoxic effect (Martin et al., 2003; Sivy et al., 2011). Alternatively, these available prenyl diphosphates could be metabolized by a prenyltransferase other than FPS, leading to the accumulation of toxic levels of pathway derivatives. In both metabolic scenarios, an external supply of MVA would be expected to exacerbate the phenotype associated with the down-regulation of FPS. However, no changes in the intensity of the phenotype were observed (Fig. 4D), which clearly ruled out the above possibilities, thus demonstrating that the phenotype of FPS-silenced plants is due to the reduced accumulation of an FPP-derived product.

The Down-Regulation of FPS Activity Disturbs Both Cytosolic and Plastidial Isoprenoid Metabolism

Analysis of the major FPP-derived end products in FPS-silenced plants revealed a similar quantitative decrease of the total amount of bulk sterols (i.e. campesterol, stigmasterol, and β-sitosterol) and UQ-9 (i.e. 30%–38% and 30% of control sterol and UQ-9 levels, respectively; Fig. 3, A and C). This is consistent with previous results showing that *fps1-1* and *fps2-1* single knockout mutants display similar, although overall less pronounced, decreases of these isoprenoids (i.e. 10%–17% and 20% of wild-type sterol and UQ-9 levels, respectively; Closa et al., 2010). Therefore, our results confirm that a limited supply of FPP has a fairly similar quantitative impact on the two major branches of the MVA-derived isoprenoid pathway, which suggests that precise regulatory mechanisms are operating to ensure a balanced distribution of FPP between these two competing pathways, particularly considering that Arabidopsis contains, by mass, about 1 order of magnitude more sterols than ubiquinones (Closa et al., 2010) and, hence, a much higher amount of FPP needs be allocated to sterol than to ubiquinone formation. The limited availability of FPP also led to qualitative changes in the profile of bulk sterols and ubiquinones. In particular, the reduction of stigmasterol was much more pronounced than that of β-sitosterol and campesterol (Fig. 3B). Such changes resulted in a drastic reduction of the stigmasterol-to-β-sitosterol ratio (i.e. more than 50% lower than in control plants), whereas the campesterol-to-β-sitosterol ratio remained unchanged. Similar qualitative changes in the profile of bulk sterols have been described in roots of Arabidopsis seedlings silenced for acetoacetyl-CoA thiolase2 (Jin et al., 2012), which catalyzes the initial reaction of the MVA pathway, and leaves of *Withania somnifera* plants silenced for SQS (Singh et al., 2015), which converts FPP into squalene, the first committed precursor of sterols and brassinosteroids (Fig. 1A). Collectively, these observations suggest that, when sterol precursors become limiting, plants keep the relative levels of campesterol and β-sitosterol properly balanced at the expense of stigmasterol to minimize the negative impact that major changes in the campesterol-to-β-sitosterol ratio might have on growth and development (Schaeffer et al., 2001). Such metabolic adaptation may involve the concerted action of highly regulated enzymes of the postsqualene segment of the sterol pathway, such as SMT2 and SMT3, the branch point isozymes starting the synthesis of structural sterols (Schaeffer et al., 2001; Carland et al., 2010), and the sterol C22 desaturase (CYP710A1) that converts β-sitosterol into stigmasterol (Morikawa et al., 2006; Arnqvist et al., 2008).

Silencing of FPS also provoked a significant change in the relative abundance of UQ-9 and UQ-10. These UQ species differ only in the length of the polyprenyl side chain, which consists of nine (C_{45}; solanesyl) and 10 (C_{50}; decaprenyl) isoprenyl units in UQ-9 and UB-10, respectively. Upon silencing of FPS, the level of UQ-10 rose up to 15% of the total UQ content, while in control plants, it accounts for only 3%. Importantly, this change is due to a decrease of UQ-9 levels concomitant to a sharp increase in the content of UQ-10 (Fig. 3C). The side chain of UQs is synthesized by trans-long-chain prenyl diphosphate synthases that elongate the allylic diphosphates FPP and GGPP by successive condensation of IPP units (Hirooka et al., 2003). The trans-long-chain prenyl diphosphate synthase that synthesizes the solanesyl side chain of UQ-9 in Arabidopsis mitochondria was recently identified and characterized (Ducluzeau et al., 2012). The enzyme shows broad product specificity with regard to chain length depending on the allylic diphosphate used as a substrate (Hsieh et al., 2011). Thus, a certain shift of the enzyme's product specificity toward longer polyprenyl diphosphates might explain the relative changes of UQ-9 and UQ-10 levels associated with FPS silencing. The limited availability of its preferred allylic substrate FPP could increase the use of GGPP as an allylic substrate for successive condensation of IPP units, thus favoring the synthesis of polyprenyl side chains of 10 units. A very recent study has demonstrated the mitochondrial localization of a GFPP-forming isoprenyl diphosphate synthase (AtIDS1) that appears also to be able to catalyze the synthesis of significant amounts of GGDP in addition to its major reaction product GFPP (Nagel et al., 2015). A similar effect on the solanesyl diphosphate synthase product chain length could be induced by a change in the ratio of the substrates FPP and IPP (Ohnuma et al., 1992; Pan et al., 2002), which is a likely consequence of the down-regulation of FPS activity. Finally, we cannot exclude the possibility that an as yet uncharacterized trans-long-chain prenyl diphosphate synthase specialized in the synthesis of the UQ-10 prenyl side chain could be up-regulated in response to the depletion of UQ-9 levels. This could be the case in tomato (*Solanum lycopersicum*) plants showing a 3-fold increase of UQ-10 levels in response to solanesyl diphosphate synthase silencing (Jones et al., 2013). Whatever the biochemical reason behind the change in the relative abundance of Arabidopsis UQ species, our results demonstrate that depletion of UQ-9 content due to a limited supply of FPP triggers a compensatory antioxidant response involving enhanced UQ-10 synthesis.

The chlorotic phenotype displayed by Arabidopsis plants silenced for FPS is most likely the result of the severe morphological and ultrastructural defects observed in their chloroplasts (Fig. 5, A and B), whose appearance resembled that of chloroplasts subjected to photooxidative damage. This is consistent with the strong depletion of chlorophylls, carotenoids, phylloquinone, plastochromanol-8, and, to a lesser extent, plastoquinone-9 observed in these plants (Fig. 5C; Supplemental Fig. S3). On the contrary, the levels of tocopherol species were unaffected or even increased (e.g. the γ-tocopherols; Supplemental Fig. S3), although this does not argue against the above, since it is becoming increasingly evident that tocopherols play a number of important biological functions beyond their

role in protecting plants from photooxidative stress, which appears to be more limited than originally assumed (Falk and Munné-Bosch, 2010). The observed increase of tocopherol content is consistent with the ultrastructural changes of chloroplasts and the concomitant chlorotic phenotype displayed by FPS-silenced plants. In fact, previous studies have indicated that the phytyl side chain of the tocopherols accumulated during chlorotic stress and leaf senescence is not synthesized de novo but formed through a salvage pathway that recycles phytol released from chlorophyll breakdown (Ischebeck et al., 2006; Vom Dorp et al., 2015). The tocopherols accumulated in plastoglobuli of chloroplasts of plants under stress have been suggested to serve as a transient sink for the deposition of phytol, which in their free form might destabilize the bilayer membrane of thylakoids due to their detergent-like characteristics (Gaude et al., 2007). The strong impact of a limited supply of cytosolic FPP on chloroplast structure and isoprenoid metabolism further reinforces the connection between cytosolic isoprenoid biosynthesis and proper plastid functioning. Therefore, plants silenced for FPS should be added to the growing list of MVA-derived isoprenoid/sterol pathway mutants displaying altered plastid-related phenotypes (Nagata et al., 2002; Suzuki et al., 2004; Babiychuk et al., 2008; Posé et al., 2009; Bouvier-Navé et al., 2010; Ishiguro et al., 2010; Kim et al., 2010).

Under the premise that the phenotype of chlorosis is due to the reduced levels of an FPP-derived isoprenoid and not to the accumulation of a toxic compound upstream of FPP, the possibility that the limited availability of an isoprenoid other than sterols may be the causative agent of such a phenotype seems unlikely. As indicated above, plant sterols are by far the most abundant FPP-derived isoprenoid products. Moreover, the external supply of *epi*-brassinolide does not restore the wild-type phenotype to FPS-silenced plants (Supplemental Fig. S2), indicating that campesterol levels (Fig. 3A) are sufficient to sustain normal brassinosteroid biosynthesis, which is in keeping with the fact that mutants defective in brassinosteroid biosynthesis and signaling are not chlorotic but darker green than wild-type plants (Fujioka et al., 1997; Li and Chory, 1997). Finally, the phenotypes of Arabidopsis mutants affected in the synthesis of other essential isoprenoids are clearly different from those of FPS-silenced plants. Plants with impaired biosynthesis of the benzenoid moiety of UQ displaying a much higher reduction in UQ content (62%) than FPS-silenced plants (Fig. 3C) are indistinguishable from wild-type plants (Block et al., 2014). Similarly, depletion of dolichol content up to 85% of the wild-type levels triggers a leaf-wilting phenotype in the margin of old leaves, but the plant growth and size are not altered significantly (Zhang et al., 2008), and Arabidopsis *era1-2* mutant plants lacking farnesyl transferase activity display enlarged organs instead of smaller ones (Yalovsky et al., 2000). These observations indicate that neither a depletion of dolichols nor defective protein farnesylation is involved in the phenotype of plants silenced for FPS. Thus, even though it is certainly possible that the flux through the branches of the isoprenoid pathway leading to FPP-derived isoprenoids other than sterols and ubiquinones also may be affected by a limited supply of FPP, the levels of the corresponding end products appear to be sufficient to sustain normal plant growth and development. The above considerations raise the question of why changes in the sterol profile may have such an important impact on chloroplast structure and function. The still controversial possibility that sterols might be required for proper biogenesis of the chloroplast membrane network should not be overlooked, as several reports claim the existence of sterols in the plastidial outer membrane of different plant species (Brandt and Benveniste, 1972; Moeller and Mudd, 1982; Hartmann-Bouillon and Benveniste, 1987; Lenucci et al., 2012), and very recently, compelling evidence supporting a direct role of sterols in chloroplast membranes was presented in the microalga *Nannochloropsis oceanica*, where, despite sterols being derived exclusively from the plastidial MEP pathway, the specific inhibition of the postsqualene sterol pathway leads to severely altered chloroplasts and depressed photosynthetic efficiency (Lu et al., 2014). Assuming that a plastid-specific sterol biosynthesis pathway in plants is highly unlikely, chloroplasts should acquire sterols from another subcellular compartment (Corbin et al., 2001) such as the ER. In fact, an extensive exchange of chemically diverse metabolites, including lipids, between the ER and plastids has been reported in many plant species, involving in some cases the establishment of physical contact sites between the membranes of these organelles (Wang and Benning, 2012; Mehrshahi et al., 2014). Thus, the depletion of sterols in plant cell membranes, including the ER network, might compromise chloroplast development, either directly because of a limited availability of sterols for deposition into plastid membranes or indirectly by altering the structure of the plastid-ER connection domains and negatively affecting the exchange of metabolites required for correct plastid metabolism and development.

Plants Perceive a Reduction of Major Sterols as a Stress Signal

The quantitative transcriptomic analyses undertaken to characterize the molecular response to the down-regulation of FPS revealed that plants perceive a reduction in the flux through the MVA-derived isoprenoid pathway and the resulting decline of sterol levels as a stress signal that causes a rapid misregulation of genes involved in both biotic and abiotic stress responses (Table I; Figs. 6, 7B, and 8). This notion is supported by the high overall degree of consistency observed when the expression changes of a targeted set of stress-related genes in response to the down-regulation of FPS were compared with those observed when the whole sterol branch of the isoprenoid

pathway was inhibited with Tb or the synthesis of structural sterols was genetically blocked (*cvp1/smt3* mutant; Fig. 7A). Thus, our RNA-seq and RT-qPCR transcriptomic analyses further strengthen the connection between distinct biotic and abiotic stresses and changes in sterol composition, in particular those affecting the stigmasterol-to-β-sitosterol ratio (Grunwald, 1978; Whitaker, 1994; Griebel and Zeier, 2010; Wang et al., 2012b; Senthil-Kumar et al., 2013; Sewelam et al., 2014), which declines sharply upon the silencing of FPS (Fig. 3B). Among the stress-related transcriptional responses, the most prominent was the induction of a set of genes related to the JA pathway, which accounted for 11.5% of the total misregulated genes and included JA biosynthesis, homeostasis, signaling, and target genes (Table I; Figs. 7B and 8A). This particular stress response also could be involved in the development of chlorosis associated with chloroplast disorganization, either by playing a primary role as a causal agent or acting synergistically with the decreased provision of sterols. JA is considered to play an important role in the initiation and progression of natural senescence, a process characterized by a gradual degreening due to the loss of chlorophyll and thylakoid membranes, and an increase in plastoglobuli (Kim et al., 2015). However, it is still unclear whether JA is a signal that triggers senescence or a by-product of senescence. It has been suggested that JA production during senescence is a consequence of increased thylakoid membrane turnover rather than the causal agent (Seltmann et al., 2010a, 2010b), and more recently, compelling evidence for the recruitment of JA biosynthetic enzymes to plastoglobuli in structurally disorganized chloroplasts has been reported in Arabidopsis mutants lacking both plastoglobule-localized kinases ABC1K1 and ABC1K3 under light stress (Lundquist et al., 2013). Thus, further work is needed in order to elucidate the actual contribution of the JA pathway to the development of the phenotypic alterations associated with the down-regulation of FPS.

In addition to the JA-related stress response, silencing of FPS also triggered changes in the expression of genes involved in abiotic stress responses (Table I; Figs. 7B and 8B). Interestingly, comparison of our results with those of transcriptomic and proteomic analyses carried out in the Arabidopsis *cyp51A2* mutant defective in the obtusifoliol-14α-demethylation step of the sterol pathway (Kim et al., 2005, 2010) revealed important differences. The JA-related stress response was not induced in this sterol-deficient mutant, which, on the other hand, exhibited an enhancement of ethylene biosynthesis and signaling and reactive oxygen species (ROS) accumulation. These responses, which have been suggested to be partly involved in the postembryonic lethality of the *cyp51A2* seedlings (Kim et al., 2005, 2010), were not activated in plants silenced for FPS (Table I; Supplemental Fig. S4B). On the contrary, genes involved in ROS detoxification were misregulated in both mutants. Thus, it can be speculated that changes in the expression of antioxidant genes in the FPS-silenced plants are able to keep ROS production and scavenging properly balanced. In any case, the observation that a perturbation of sterol homeostasis may result in substantially different molecular responses is not unprecedented. Silencing of SQS in *W. somnifera* results in reduced sterol levels and leads to decreased expression of both JA-dependent PR3 and SA-dependent PR1 and PR5 transcripts (Singh et al., 2015), while the expression of *Brassica juncea* HMG-CoA synthase in Arabidopsis increases the sterol content and activates the expression of the SA-dependent PR1, PR2, and PR5 transcripts with no involvement of the JA pathway in the defense response (Wang et al., 2012a). However, neither the SA nor the JA defense pathway is activated in *Pseudomonas syringae*-resistant Arabidopsis mutants lacking sterol C22 desaturase (CYP710A1) activity (Griebel and Zeier, 2010). So far, the reasons behind these differential stress responses to changes in the profile of sterols are unknown, but it may reflect specific differences in the relative abundance of individual sterols in each of these mutants. The precise mechanism by which the relative amounts of plant sterols, in combination with other membrane lipids, finely control the physicochemical properties of membranes and their biological function is still unclear, but it is known that the contribution of individual sterols to the biophysical properties and the functionality of cell membranes and the associated proteins differs greatly (Schuler et al., 1991; Grandmougin-Ferjani et al., 1997; Hartmann, 1998; Hodzic et al., 2008; Grosjean et al., 2015). The fact that particular sterol imbalances may have specific consequences also could explain the minor differences observed in the gene expression patterns depending on whether sterol biosynthesis was inhibited at the level of FPS or downstream in the pathway and even the intriguing observation that some sterol biosynthetic mutants do not display plastid-related phenotypes (Carland et al., 2010; Jin et al., 2012).

Reduced Levels of Major Sterols Alter Fe Homeostasis

In plants silenced for FPS, transcripts coding for proteins involved in Fe storage, metabolism, and/or intracellular trafficking were down-regulated, whereas those coding for group Ib bHLH transcription factors known to play essential roles in activating Fe deficiency responses and uptake were up-regulated (Table I; Fig. 7B). This Fe deficiency transcriptional response is consistent with the reduced levels of Fe measured in FPS-silenced plants (Fig. 9B) and also was observed when the sterol branch of the isoprenoid pathway was inhibited (Fig. 7B). These results confirmed the existence of a close relationship between plant sterol metabolism and Fe homeostasis, a connection that is well established in other organisms such as fungi (Craven et al., 2007; Blatzer et al., 2011; Hosogaya et al., 2013; Thomas et al., 2013; Chung et al., 2014; Vasicek et al., 2014) but is much less known in plants (Urbany et al., 2013). In general, depletion of sterol biosynthesis has

been correlated with both higher membrane permeability and increased uptake of metal ions in roots, although the underlying molecular mechanism remains unknown (Diener et al., 2000; Khan et al., 2009; Urbany et al., 2013; Wagatsuma et al., 2015). These observations argue against the possibility that the Fe deficiency-related gene expression response may be a direct consequence of the impact of reduced sterol levels on membrane permeability. The suggested role of JA as a negative regulator of Fe deficiency gene expression (Hindt and Guerinot, 2012) further reinforces this hypothesis, as silencing of FPS triggers a JA-related transcriptional response. Thus, considering that the vast majority of leaf cellular Fe is stored in the chloroplasts associated with metalloproteins of the thylakoid electron transfer chain (Briat et al., 2007), a most plausible hypothesis could be that the altered Fe homeostasis in response to the down-regulation of FPS results from the strong impact of this metabolic perturbation on chloroplast size and structural integrity (Fig. 5, A and B). The impact of FPS down-regulation on chloroplasts also might be the underlying cause of changes in the expression of genes coding for proteins involved in carbohydrate metabolism (Table I; Fig. 7B).

CONCLUSION

The presented results indicate that Arabidopsis plants silenced for FPS develop a chlorotic phenotype associated with important morphological and structural alterations of chloroplasts and a marked change in the profile of both cytosolic and plastidial isoprenoids, including a depletion of the bulk membrane sterols, which is perceived by plants as a stress signal that induces early transcriptional stress responses, including JA signaling and Fe homeostasis. This supports the view that plant sterol levels must be stringently controlled and indicates that changes in the composition of sterols are rapidly sensed by plant cells, which in turn activate a series of adaptive responses aimed at coping with the new metabolic scenario. Further studies are required to determine the role and mode of action of individual sterol species, paying special attention to the emerging connection between sterol metabolism and chloroplasts, which appears to be a key player of this complex regulatory response.

MATERIALS AND METHODS

Plant Growth Conditions and Treatments

Arabidopsis (*Arabidopsis thaliana*) plants of ecotype Col-0 were used throughout this study. For in vitro culture, seeds were surface sterilized with ethanol and sown on petri dishes containing MS medium (MS salts, 1% [w/v] Suc, and 0.8% [w/v] agar, pH 5.7). After stratification at 4°C for 2 d, plates were transferred into a growth chamber set for long-day conditions (16 h of light/8 h of darkness) at 150 μmol m^{-2} s^{-1} and 22°C. To induce *FPS* gene silencing, seedlings were germinated and grown on MS medium supplemented with 30 μM MFZ (Runner; Bayer CropScience) or germinated and grown for 3 d on sterile filter papers that were first placed on MS plates and subsequently transferred onto new MS plates supplemented or not with 30 μM MFZ. For phenotype reversion experiments, seedlings were germinated and grown as indicated above on growth medium supplemented with 5 mM MVA (Sigma M4667) or 0.4 nM *epi*-brassinolide (Wako). For chemical inhibition of the sterol pathway, 3-d-old seedlings grown on filter papers on MS medium were transferred to new MS plates supplemented or not with 150 μM Tb (Sigma T8826). The *cvp1/smt3* double mutant plants (Carland et al., 2010), kindly provided by Dr. Francine Carland, were grown for 8 d in the same conditions. In all cases, seedlings were grown for the desired time intervals under the light and temperature conditions indicated above. Seedling samples were collected in three biological replicates, quickly frozen in liquid nitrogen, and stored at −80°C until further processing.

Generation of Pre-amiRNA DNA Vectors and Plant Transformation

Two amiRNA sequences (amiFPSa and amiFPSb) were designed to target simultaneously *FPS1* and *FPS2* genes (Fig. 1B) using the Web MicroRNA Designer (http://wmd3.weigelworld.org/cgi-bin/webapp.cgi; Schwab et al., 2006; Ossowski et al., 2008). The amiRNA fold-back fragments were generated by overlap PCR using pRS300 plasmid as a template and the following oligonucleotides: FPSaI (5′-gaTATTGCGAAGTAGAATCGCGTtctctcttttgtattcc-3′), FPSaII (5′-gaACGCGATTCTACTTCGCAATAtcaaagagaatcaatga-3′), FPSaIII (5′-gaACACGATTCTACTACGCAATTtcacaggtcgtgatatg-3′), and FPSaIV (5′-gaAATTGCGTAGTAGAATCGTGTtctacatatatattcct-3′) for amiFPSa and FPSbI (5′-gaTAGGTCAACATAGTAAGCCTTtctctcttttgtattcc-3′), FPSbII (5′-gaAAGGCTTACTATGTTGACCTAtcaaagagaatcaatga-3′), FPSbIII (5′-gaAAAGCTTACTATGATGACCTTtcacaggtcgtgatatg-3′), and FPSbIV (5′-gaAAGGTCATCATAGTAAGCTTTctacatatatattcct-3′) for amiFPSb.

The amplified fragments were gel purified and cloned into pGEM-T Easy vector (Promega). After sequencing to exclude amplification artifacts, the pre-amiFPSa and pre-amiFPSb constructs were digested with *Sal*I and *Not*I and subcloned into the pENTR3C Gateway entry vector (Life Technologies). The resulting pre-amiFPS constructs were then transferred into pB110-Red-2844 binary vector harboring the ecdysone-inducible receptor-based system (Padidam et al., 2003) using Gateway LR Clonase II Enzyme mix (Invitrogen). An empty version of pB100-Red-2844 (EV) to generate EV plants that were used as a control in FPS-silencing experiments was generated as follows. Plasmid pENTR3C was digested with *Eco*RI, religated to eliminate the *ccdB* gene, and subsequently recombined into pB100-Red-2844 using LR Clonase reaction to yield pB100-Red-EV. The recombinant binary plasmids were transferred to *Agrobacterium tumefaciens* strain GV3101, and the resulting strains were used to transform Arabidopsis Col-0 plants by the floral dip method (Clough and Bent, 1998). Transformed plant lines homozygous for the corresponding transgenes were selected on the basis of the segregation of the red fluorescence trait in transgenic seeds. Transgenic Arabidopsis homozygous for the pre-amiFPSa MFZ-inducible transgene were retransformed with a 35S::FPS1S gene construct devised for constitutive overexpression of the Arabidopsis FPS1S isoform (Masferrer et al., 2002) as indicated above. Double homozygous transgenic lines were selected using the kanamycin resistance trait. T3 plants were genotyped by PCR for the presence of the 35S::FPS1S transgene using primer pair 35S-3′F (5′-CACTGACGTAAGGGATGACG-3′) and FPS1Srv (5′-CTGTGGATGTGATTGCGAAGTAG-3′) and for the presence of the amiFPSa construct using primer pair FPSaII and FPSaIII. PCR was performed using genomic DNA with a melting temperature for the annealing step of 55°C and 35 cycles. The amiFPSa RNA levels were quantified in double and single transgenic plants by reverse transcription-PCR as described elsewhere (Varkonyi-Gasic et al., 2007) using the following oligonucleotides: RT-amiRFPSa (5′-GTCGTATCCAGTGCAGGGTCCGAGGTATTCGCACTGGATACGACAC-GCGA-3′) for amiRNA-specific reverse transcription and microUNI-rv (5′-CCAGTGCAGGGTCCGAGGTA-3′) and amiRFPSa-fw (5′-CAGGCATAT-TGCGAAGTAGAATC-3′) for PCR amplification.

Laser Confocal Microscopy

For chloroplast observation, whole seedlings were examined by confocal laser scanning microscopy using a Leica SP5II microscope (Leica Microsystems) and a water-immersion objective (HCX PL Apo 63×/1.20 W). Chlorophyll fluorescence was excited with an argon laser at 488 nm and detected using a 640- to 680-nm band-pass filter. LAS-AF Lite 2.6.0 software was used for image capture. Chloroplast area was measured using confocal microscopy images and ImageJ software (Image Processing and Analysis in Java; http://imagej.nih.gov/ij/). Thirty-six independent chloroplast measurements were made for each plant line and treatment.

Transmission Electron Microscopy

For electron microscopy, the first pair of true leaves from seedlings were cut into small pieces and fixed with a mixture of 2% paraformaldehyde and 2.5% glutaraldehyde in 0.1 M phosphate buffer (pH 7.4) overnight at 4°C. Samples were then washed with phosphate buffer, postfixed with 2% (w/v) OsO_4 for 2 h, and sequentially washed again with MilliQ water and phosphate buffer during 10 min each. Sections were dehydrated at 4°C through a series of increasing acetone concentrations (50%, 70%, 90%, 96%, and 100%) prior to being progressively (25%, 50%, 75%, and 100%) embedded in Epon 812 epoxy resin. The resin was polymerized at 60°C during 48 h. Sections with a thickness of 50 nm were cut with an ultramicrotome (UC6; Leica Microsystems) and placed on transmission electron microscopy grids (Formvar carbon-coated copper grids). Finally, grids were further contrasted with uranyl acetate and lead citrate. All electron micrographs were obtained with a JEOL JEM 1010 MT electron microscope operating at 80 kV. Images were recorded with AnalySIS on a Megaview III CCD camera.

Western-Blot Analysis and Enzyme Activity Assays

Seedling extracts for HMGR and FPS activity assays were obtained as described by Campos et al. (2014) and Arró et al. (2014), respectively. HMGR activity was determined as described by Campos et al. (2014) and is reported as picomoles of 3-HMG-CoA converted into MVA per minute per milliliter of protein extract at 37°C. FPS activity was measured as described by Arró et al. (2014) and is reported as picomoles of IPP incorporated into acid-labile products per minute per milliliter of protein extract at 37°C. Immunoblot analysis was performed as described by Keim et al. (2012) in the same protein extracts used for enzyme activity assays. Protein samples corresponding to 7 and 2 μL of each of the extracts analyzed for FPS and HMGR activity levels, respectively, were loaded into gel lanes. Rabbit polyclonal antibodies raised against FPS1 (Masferrer et al., 2002) and HMGR1 (Manzano et al., 2004) were used at 1:8,000 and 1:20,000 dilutions, respectively. The secondary antibody (goat anti-rabbit IgG conjugated to horseradish peroxidase) was used at a 1:50,000 dilution. The FPS and HMGR antibody complexes were visualized using the ECL Advance western-blotting system (GE Healthcare) according to the manufacturer's instructions. Protein concentration was determined as described by Bradford (1976), and the amount of protein on the blotted membranes was assessed by Coomassie Blue staining.

Metabolite Analysis

A pool of 100 mg fresh weight of seedlings per genotype and treatment was used for each measurement, and all the measurements were carried out in three independent biological replicates. Quantification of sterols was performed by gas chromatography-mass spectrometry as described previously (Closa et al., 2010). For photosynthetic pigment analysis, seedling samples were immediately frozen in liquid nitrogen and ground to a fine powder using TissueLyser equipment. Photosynthetic pigments were extracted in 1 mL of 80% acetone in the dark at 4°C for 1 h. Plant extracts were centrifuged for 5 min at 13,000 rpm at 4°C, and the supernatant was subjected to spectrophotometric analysis at 470, 646, and 663 nm. The chlorophyll *a* and *b*, total chlorophyll, and carotenoid contents were calculated as described by Lichtenthaler (1987). Quantitative analysis of prenylquinones and carotenoids was performed by ultra-performance liquid chromatography-mass spectrometry as described using 30 to 45 mg dry weight of seedlings (Martinis et al., 2011; Kessler and Glauser, 2014). Absolute quantification of phylloquinone, plastochromanol-8, plastoquinone-9, and tocopherol levels was made using the corresponding standards, and values are reported in micrograms per gram dry weight. Ubiquinone-9, ubiquinone-10, β-carotene, lutein, and violaxanthin-neoxanthin levels are reported as relative amounts that were calculated using the value of the signal divided by the mass of samples.

RNA-Seq and Differential Gene Expression Analysis

RNA Preparation and Illumina Sequencing

For RNA-seq, amiFPSa plants were grown on MS medium or MS medium supplemented with 30 μM MFZ. Three independent pools of seedlings (100 mg fresh weight) were collected for each treatment. Seedlings were ground to a fine powder using TissueLyser equipment and used for the extraction of RNA using NucleoSpin RNA Plant (Macherey-Nagel) according to the manufacturer's instructions, including the DNase step. The quality and quantity of total RNA samples were assessed using a Bionalyzer Expert 2100 Instrument (Agilent Technologies), and an equimolar mixture of RNA samples from each treatment was prepared. The RNA samples (3 μg) were fragmented and ligated with adaptors prior to cDNA synthesis and PCR amplification. The cDNA libraries were prepared according to Illumina protocols and sequenced using an Illumina HiSeq 2000 machine to perform 2 $\times$ 100 paired-end sequencing.

Mapping and Differential Gene Expression Analysis

The quality of the reads obtained by HiSeq 2000 sequencing was checked with FastQC software (http://www.bioinformatics.bbsrc.ac.uk/projects/fastqc/). Preprocessing of the reads was performed with fastx-toolkit (http://hannonlab.cshl.edu/fastx_toolkit/index.html) and aScidea specific perl scripts (http://www.ascidea.com) in order to filter regions of low quality. Adaptors and low-quality bases at the ends of sequences and reads with undetermined bases or with 80% of their bases with less than 20% quality score were trimmed, and raw reads that passed the quality filter threshold were mapped using Tophat 2.0.7 (Trapnell et al., 2009) and Bowtie 2 2.0.6 (Langmead et al., 2009; Langmead and Salzberg, 2012) to generate read alignments for each sample. The reference genome used was TAIR 10, and genomic annotations were obtained from TAIR (http://www.arabidopsis.org) in general feature format 3. The inner distance between mate pairs used was 50 bp, and the rest of the parameters were used with the default values. The transcript isoform level and gene level counts were calculated and fragments per kilobase of exon per million fragments mapped normalized using Cufflinks 2.0.2 software (Trapnell et al., 2010). Differential transcript expression was then computed using Cuffdiff (Trapnell et al., 2013). The resulting lists of differentially expressed genes were filtered by $\log_2$ (fold change) greater than 2 and less than -2 and a q value of 0.05. The analysis of biological significance was based on Gene Ontology (Ashburner et al., 2000) using the hypergeometric statistical test and the Bonferroni multitest adjustment method considering a significance level cutoff of 0.05. Gene Ontology was performed using GeneCodis (Carmona-Saez et al., 2007; Nogales-Cadenas et al., 2009) Web services. The main statistical analyses were performed using the free statistical language R and the libraries developed for data analysis by the Bioconductor project (www.bioconductor.org). Raw data of the experiment can be downloaded from the Gene Expression Omnibus (http://www.ncbi.nlm.nih.gov/geo/) with accession number GSE79412.

Fe Quantification

For the quantification of Fe levels, seedlings were collected and freeze dried overnight. About 30 to 45 mg of dry material was digested with 1 mL of HNO_3 and 0.5 mL of hydrogen peroxide overnight at 90°C. After cooling down, 10 mL of ultra-pure water was added. Fe content was measured using an inductively coupled plasma optical emission spectrometer (Optima 3200 RL; Perkin-Elmer). Analyses of samples followed external calibration with a diluted single Fe element. The total Fe concentration of seedlings of the different lines analyzed was determined in biological triplicates from independent experiments. One-way ANOVA was performed using Graphpad Prism (version 5) software.

RT-qPCR Analysis of HMG and FPS Gene Expression

Total RNA was extracted from seedling samples (100 mg fresh weight) using the PureLink RNA Mini Kit (Ambion, Life Technologies) following the manufacturer's instructions. The RNA samples were treated with DNase I (DNA-free kit; Ambion) in a final reaction volume of 25 μL, and cDNA was synthesized from 1 μg of total RNA using SuperScript III Reverse Transcriptase (Invitrogen) and oligo(dT) primers. Real-time PCR was performed using LightCycler 480 equipment (Roche Diagnostics). The raw PCR data from LightCycler software 1.5.0 were used in the analysis. Amplification curves were analyzed using the second derivative maximum method, and crossing points were determined for each curve. For efficiency determination, a standard curve of six serial dilution points (ranging from 200 to 6.25 ng) was made in triplicate. Specific primer pairs for HMG1 and HMG2 mRNAs were described previously (Nieto et al., 2009). The following specific primer pairs were used for FPS1 and FPS2 mRNAs: qFPS1fw (5′-AAAGTCTCAGCCCTCAAAAATTTC-3′), qFPS1rv (5′-CAAGAATAAAAGTGAGGCAGGTTT-3′), qFPS2fw (5′-CGTTTTATTC-TTCTGACATTTATGTAT-3′), and qFPS2rv (5′-AATCTCAAATTCTATTTTC-GGAAGG-3′). Quantification of transcript levels was done in three independent biological replicates, and for each biological replicate, three

technical replicates were performed. *PP2AA3* (At1g13320) was used as a housekeeping gene with previously designed oligonucleotides (Hong et al., 2010). The cycle threshold change (ΔCT) was calculated as follows: ΔCT = CT (Target) − CT (PP2A). The fold change value was calculated using the expression 2 − ΔCT (Livak and Schmittgen, 2001).

High-Throughput RT-qPCR Gene Expression Analysis

RNA extraction and cDNA synthesis were performed as described above for standard RT-qPCR analysis. Transgene expression was quantified by real-time PCR using a BioMark HD instrument (Fluidigm; www.fluidigm.com) and 2× SsoFast EvaGreen Supermix with low Rox (Bio-Rad; www.bio-rad.com) dye. The cDNA samples were diluted from 0.15 to 6 ng μL^{-1} and preamplified using TaqMan PreAmp Master Mix (Applied Biosystems, Life Technologies). Primers were used at a final concentration of 500 nM. After preamplification, cDNAs were treated with exonuclease I to remove leftover primers. Primer pairs for each gene candidate were designed using PrimerQuest (http://eu.idtdna.com/PrimerQuest/Home/Index; for a complete list of oligonucleotides, see Supplemental Table S2). The PCR efficiency for each primer pair used was calculated according to a dilution series from a pooled cDNA sample including all biological treatments. Expression fold was calculated using DAG Expression software (http://www.dagexpression.com/dage.zip; Ballester et al., 2013) through the construction of standard curves for relative quantification and multiple reference genes for sample normalization. Quantification of transcript levels was done in three independent biological replicates, and for each biological replicate, two technical replicates were performed. Three different reference genes reported previously as stably expressed during plant development and throughout time-course experiments were selected: *PP2AA3* (At1g13320), *UBC9* (At4g27960; Hong et al., 2010), and *UBC* (At5g25760; Czechowski et al., 2005).

Hierarchical Clusterization

Hierarchical clusterization of the genes was performed using the TM4 suite (http://www.tm4.org/mev.html). The clusterization was performed using the Euclidean distance of the gene expression profiles across the different comparisons, and the average clusterization method was used (Eisen et al., 1998).

Data Analysis

The statistical significance of changes between amiFPS and EV plants grown on MS medium supplemented with MFZ was calculated using paired Student's *t* tests.

Accession Numbers

Raw sequencing data and processed sequence data from the RNAseq experiment are stored at the Gene Expression Omnibus (http://www.ncbi.nlm.nih.gov/geo/) under accession number GSE79412.

Supplemental Data

The following supplemental materials are available.

Supplemental Figure S1. Overexpression of FPS1S restores the wild-type phenotype to silenced plants.

Supplemental Figure S2. Brassinosteroids fail to complement the phenotypes caused by silencing of FPS.

Supplemental Figure S3. Effect of FPS silencing on carotenoid and prenylquinone levels.

Supplemental Figure S4. Silencing of FPS leads to the misregulation of genes involved in maintaining redox homeostasis but does not trigger symptoms of oxidative stress.

Supplemental Figure S5. Time-course expression analysis of genes coding for enzymes involved in carbohydrate metabolism.

Supplemental Table S1. Transcriptomic analysis of FPS-silenced plants using Illumina RNA-seq technology.

Supplemental Table S2. List of oligonucleotides used in high-throughput quantitative PCR gene expression analysis (BioMark system from Fluidigm).

ACKNOWLEDGMENTS

We thank Dr. Francine Carland (Yale University) for *cvp1/smt3* mutant plants and Dr. Ming Chen and Dr. Edgar B. Cahoon (Donald Danforth Plant Science Center) for the pB110-Red-2844 plasmid; Dr. Detlef Weigel for providing the amiRNA system; Manuel Castro (Ascidea) for bioinformatic analysis of the RNA-seq data and Dr. Riccardo Aiese Cigliano (Sequentia) for help with the hierarchical clustering analysis; Dr. Maria Ballester (Institut de Recerca i Tecnologia Alimentària) for support with the differential gene expression analysis software; the greenhouse facilities, the Scientific and Technical Services at the Centre for Research in Agricultural Genomics, and the Centres Científics i Tecnològics of the University of Barcelona; Manuel Rodríguez-Concepción and Norma Fàbregas for critical reading of the article; and Berta Esteve and Antonella Pavoni for technical help. We acknowledge financial support from the Spanish Ministry of Economy and Competitiveness through the "Severo Ochoa Programme for Centres of Excellence in R&D" 2016-2019 (SEV-2015-0533).

Received March 18, 2016; accepted June 30, 2016; published July 5, 2016.

LITERATURE CITED

Al-Babili S, Bouwmeester HJ (2015) Strigolactones, a novel carotenoid-derived plant hormone. Annu Rev Plant Biol **66:** 161–186

Arnqvist L, Persson M, Jonsson L, Dutta PC, Sitbon F (2008) Overexpression of CYP710A1 and CYP710A4 in transgenic Arabidopsis plants increases the level of stigmasterol at the expense of sitosterol. Planta **227:** 309–317

Arró M, Manzano D, Ferrer A (2014) Farnesyl diphosphate synthase assay. Methods Mol Biol **1153:** 41–53

Ashburner M, Ball CA, Blake JA, Botstein D, Butler H, Cherry JM, Davis AP, Dolinski K, Dwight SS, Eppig JT, et al (2000) Gene Ontology: tool for the unification of biology. Nat Genet **25:** 25–29

Babiychuk E, Bouvier-Navé P, Compagnon V, Suzuki M, Muranaka T, Van Montagu M, Kushnir S, Schaller H (2008) Allelic mutant series reveal distinct functions for Arabidopsis cycloartenol synthase 1 in cell viability and plastid biogenesis. Proc Natl Acad Sci USA **105:** 3163–3168

Ballester M, Cordón R, Folch JM (2013) DAG expression: high-throughput gene expression analysis of real-time PCR data using standard curves for relative quantification. PLoS ONE **8:** e80385

Beck JG, Mathieu D, Loudet C, Buchoux S, Dufourc EJ (2007) Plant sterols in "rafts": a better way to regulate membrane thermal shocks. FASEB J **21:** 1714–1723

Benveniste P (2004) Biosynthesis and accumulation of sterols. Annu Rev Plant Biol **55:** 429–457

Bhatia V, Maisnam J, Jain A, Sharma KK, Bhattacharya R (2015) Aphid-repellent pheromone E-β-farnesene is generated in transgenic Arabidopsis thaliana over-expressing farnesyl diphosphate synthase2. Ann Bot (Lond) **115:** 581–591

Bick JA, Lange BM (2003) Metabolic cross talk between cytosolic and plastidial pathways of isoprenoid biosynthesis: unidirectional transport of intermediates across the chloroplast envelope membrane. Arch Biochem Biophys **415:** 146–154

Blatzer M, Barker BM, Willger SD, Beckmann N, Blosser SJ, Cornish EJ, Mazurie A, Grahl N, Haas H, Cramer RA (2011) SREBP coordinates iron and ergosterol homeostasis to mediate triazole drug and hypoxia responses in the human fungal pathogen Aspergillus fumigatus. PLoS Genet **7:** e1002374

Block A, Widhalm JR, Fatihi A, Cahoon RE, Wamboldt Y, Elowsky C, Mackenzie SA, Cahoon EB, Chapple C, Dudareva N, et al (2014) The origin and biosynthesis of the benzenoid moiety of ubiquinone (coenzyme Q) in *Arabidopsis*. Plant Cell **26:** 1938–1948

Bohlmann J, Keeling CI (2008) Terpenoid biomaterials. Plant J **54:** 656–669

Bouvier-Navé P, Berna A, Noiriel A, Compagnon V, Carlsson AS, Banas A, Stymne S, Schaller H (2010) Involvement of the phospholipid sterol acyltransferase1 in plant sterol homeostasis and leaf senescence. Plant Physiol **152:** 107–119

Bradford MM (1976) A rapid and sensitive method for the quantitation of microgram quantities of protein utilizing the principle of protein-dye binding. Anal Biochem **72:** 248–254

Brandt RD, Benveniste P (1972) Isolation and identification of sterols from subcellular fractions of bean leaves (Phaseolus vulgaris). Biochim Biophys Acta **282:** 85–92

Briat JF, Curie C, Gaymard F (2007) Iron utilization and metabolism in plants. Curr Opin Plant Biol **10:** 276–282

Briat JF, Duc C, Ravet K, Gaymard F (2010) Ferritins and iron storage in plants. Biochim Biophys Acta **1800:** 806–814

Campbell EJ, Schenk PM, Kazan K, Penninckx IA, Anderson JP, Maclean DJ, Cammue BPA, Ebert PR, Manners JM (2003) Pathogen-responsive expression of a putative ATP-binding cassette transporter gene conferring resistance to the diterpenoid sclareol is regulated by multiple defense signaling pathways in Arabidopsis. Plant Physiol **133:** 1272–1284

Campos N, Arró M, Ferrer A, Boronat A (2014) Determination of 3-hydroxy-3-methylglutaryl CoA reductase activity in plants. Methods Mol Biol **1153:** 21–40

Carland F, Fujioka S, Nelson T (2010) The sterol methyltransferases SMT1, SMT2, and SMT3 influence Arabidopsis development through nonbrassinosteroid products. Plant Physiol **153:** 741–756

Carland FM, Fujioka S, Takatsuto S, Yoshida S, Nelson T (2002) The identification of CVP1 reveals a role for sterols in vascular patterning. Plant Cell **14:** 2045–2058

Carmona-Saez P, Chagoyen M, Tirado F, Carazo JM, Pascual-Montano A (2007) GENECODIS: a web-based tool for finding significant concurrent annotations in gene lists. Genome Biol **8:** R3

Carruthers A, Melchoir DL (1986) How bilayer lipids affect membrane-protein activity. Trends Biochem Sci **11:** 331–335

Chen F, Tholl D, Bohlmann J, Pichersky E (2011) The family of terpene synthases in plants: a mid-size family of genes for specialized metabolism that is highly diversified throughout the kingdom. Plant J **66:** 212–229

Chung D, Barker BM, Carey CC, Merriman B, Werner ER, Lechner BE, Dhingra S, Cheng C, Xu W, Blosser SJ, et al (2014) ChIP-seq and in vivo transcriptome analyses of the Aspergillus fumigatus SREBP SrbA reveals a new regulator of the fungal hypoxia response and virulence. PLoS Pathog **10:** e1004487

Closa M, Vranová E, Bortolotti C, Bigler L, Arró M, Ferrer A, Gruissem W (2010) The Arabidopsis thaliana FPP synthase isozymes have overlapping and specific functions in isoprenoid biosynthesis, and complete loss of FPP synthase activity causes early developmental arrest. Plant J **63:** 512–525

Clough SJ, Bent AF (1998) Floral dip: a simplified method for Agrobacterium-mediated transformation of Arabidopsis thaliana. Plant J **16:** 735–743

Cooke DJ, Burden RS (1990) Lipid modulation of plasma-membrane-bound ATPases. Physiol Plant **78:** 153–159

Corbin DR, Grebenok RJ, Ohnmeiss TE, Greenplate JT, Purcell JP (2001) Expression and chloroplast targeting of cholesterol oxidase in transgenic tobacco plants. Plant Physiol **126:** 1116–1128

Craven RJ, Mallory JC, Hand RA (2007) Regulation of iron homeostasis mediated by the heme-binding protein Dap1 (damage resistance protein 1) via the P450 protein Erg11/Cyp51. J Biol Chem **282:** 36543–36551

Croteau R, Kutchan TM, Lewis NG (2000) Natural products (secondary metabolites). *In* B Buchanan, W Gruissem, R Jones, eds, Biochemistry and Molecular Biology of Plants. American Society of Plant Physiologists, Rockville, MD, pp 1250–1318

Crowell DN, Salaz MS (1992) Inhibition of growth of cultured tobacco cells at low concentrations of lovastatin is reversed by cytokinin. Plant Physiol **100:** 2090–2095

Cunillera N, Arró M, Delourme D, Karst F, Boronat A, Ferrer A (1996) Arabidopsis thaliana contains two differentially expressed farnesyl-diphosphate synthase genes. J Biol Chem **271:** 7774–7780

Cunillera N, Boronat A, Ferrer A (1997) The Arabidopsis thaliana FPS1 gene generates a novel mRNA that encodes a mitochondrial farnesyl-diphosphate synthase isoform. J Biol Chem **272:** 15381–15388

Czechowski T, Stitt M, Altmann T, Udvardi MK, Scheible WR (2005) Genome-wide identification and testing of superior reference genes for transcript normalization in Arabidopsis. Plant Physiol **139:** 5–17

Dale S, Arró M, Becerra B, Morrice NG, Boronat A, Hardie DG, Ferrer A (1995) Bacterial expression of the catalytic domain of 3-hydroxy-3-methylglutaryl-CoA reductase (isoform HMGR1) from Arabidopsis thaliana, and its inactivation by phosphorylation at Ser577 by Brassica oleracea 3-hydroxy-3-methylglutaryl-CoA reductase kinase. Eur J Biochem **233:** 506–513

Diener AC, Li H, Zhou W, Whoriskey WJ, Nes WD, Fink GR (2000) Sterol methyltransferase 1 controls the level of cholesterol in plants. Plant Cell **12:** 853–870

Dietrich CR, Han G, Chen M, Berg RH, Dunn TM, Cahoon EB (2008) Loss-of-function mutations and inducible RNAi suppression of Arabidopsis LCB2 genes reveal the critical role of sphingolipids in gametophytic and sporophytic cell viability. Plant J **54:** 284–298

Disch A, Hemmerlin A, Bach TJ, Rohmer M (1998) Mevalonate-derived isopentenyl diphosphate is the biosynthetic precursor of ubiquinone prenyl side chain in tobacco BY-2 cells. Biochem J **331:** 615–621

Dixon DP, Skipsey M, Edwards R (2010) Roles for glutathione transferases in plant secondary metabolism. Phytochemistry **71:** 338–350

Doblas VG, Amorim-Silva V, Posé D, Rosado A, Esteban A, Arró M, Azevedo H, Bombarely A, Borsani O, Valpuesta V, et al (2013) The SUD1 gene encodes a putative E3 ubiquitin ligase and is a positive regulator of 3-hydroxy-3-methylglutaryl coenzyme A reductase activity in *Arabidopsis*. Plant Cell **25:** 728–743

Douglas P, Pigaglio E, Ferrer A, Halfords NG, MacKintosh C (1997) Three spinach leaf nitrate reductase-3-hydroxy-3-methylglutaryl-CoA reductase kinases that are regulated by reversible phosphorylation and/or Ca^{2+} ions. Biochem J **325:** 101–109

Ducluzeau AL, Wamboldt Y, Elowsky CG, Mackenzie SA, Schuurink RC, Basset GJC (2012) Gene network reconstruction identifies the authentic trans-prenyl diphosphate synthase that makes the solanesyl moiety of ubiquinone-9 in Arabidopsis. Plant J **69:** 366–375

Dyson BC, Allwood JW, Feil R, Xu Y, Miller M, Bowsher CG, Goodacre R, Lunn JE, Johnson GN (2015) Acclimation of metabolism to light in Arabidopsis thaliana: the glucose 6-phosphate/phosphate translocator GPT2 directs metabolic acclimation. Plant Cell Environ **38:** 1404–1417

Eisen MB, Spellman PT, Brown PO, Botstein D (1998) Cluster analysis and display of genome-wide expression patterns. Proc Natl Acad Sci USA **95:** 14863–14868

Enjuto M, Balcells L, Campos N, Caelles C, Arró M, Boronat A (1994) Arabidopsis thaliana contains two differentially expressed 3-hydroxy-3-methylglutaryl-CoA reductase genes, which encode microsomal forms of the enzyme. Proc Natl Acad Sci USA **91:** 927–931

Falk J, Munné-Bosch S (2010) Tocochromanol functions in plants: antioxidation and beyond. J Exp Bot **61:** 1549–1566

Flügge UI, Gao W (2005) Transport of isoprenoid intermediates across chloroplast envelope membranes. Plant Biol (Stuttg) **7:** 91–97

Foyer CH, Noctor G (2011) Ascorbate and glutathione: the heart of the redox hub. Plant Physiol **155:** 2–18

Fujiki Y, Ito M, Nishida I, Watanabe A (2000) Multiple signaling pathways in gene expression during sugar starvation: pharmacological analysis of din gene expression in suspension-cultured cells of Arabidopsis. Plant Physiol **124:** 1139–1148

Fujiki Y, Yoshikawa Y, Sato T, Inada N, Ito M, Nishida I, Watanabe A (2001) Dark-inducible genes from Arabidopsis thaliana are associated with leaf senescence and repressed by sugars. Physiol Plant **111:** 345–352

Fujioka S, Li J, Choi YH, Seto H, Takatsuto S, Noguchi T, Watanabe T, Kuriyama H, Yokota T, Chory J, et al (1997) The *Arabidopsis deetiolated2* mutant is blocked early in brassinosteroid biosynthesis. Plant Cell **9:** 1951–1962

Fujioka S, Yokota T (2003) Biosynthesis and metabolism of brassinosteroids. Annu Rev Plant Biol **54:** 137–164

Gas-Pascual E, Simonovik B, Schaller H, Bach TJ (2015) Inhibition of cycloartenol synthase (CAS) function in tobacco BY-2 cells. Lipids **50:** 761–772

Gaude N, Bréhélin C, Tischendorf G, Kessler F, Dörmann P (2007) Nitrogen deficiency in Arabidopsis affects galactolipid composition and gene expression and results in accumulation of fatty acid phytyl esters. Plant J **49:** 729–739

George KW, Alonso-Gutierrez J, Keasling JD, Lee TS (2015) Isoprenoid drugs, biofuels, and chemicals: artemisinin, farnesene, and beyond. Adv Biochem Eng Biotechnol **148:** 355–389

Grandmougin-Ferjani A, Schuler-Muller I, Hartmann MA (1997) Sterol modulation of the plasma membrane H^+-ATPase activity from corn roots reconstituted into soybean lipids. Plant Physiol **113:** 163–174

Griebel T, Zeier J (2010) A role for β-sitosterol to stigmasterol conversion in plant-pathogen interactions. Plant J **63:** 254–268

Grosjean K, Mongrand S, Beney L, Simon-Plas F, Gerbeau-Pissot P (2015) Differential effect of plant lipids on membrane organization: specificities of phytosphingolipids and phytosterols. J Biol Chem **290:** 5810–5825

Grunwald C (1978) Shading influence on the sterol balance of *Nicotiana tabacum* L. Plant Physiol **61:** 76–79

Hartmann MA (1998) Plant sterols and the membrane environment. Trends Plant Sci **3:** 170–175

Hartmann-Bouillon MA, Benveniste P (1987) Plant membrane sterols: isolation, identification and biosynthesis. Methods Enzymol **148:** 632–650

He JX, Fujioka S, Li TC, Kang SG, Seto H, Takatsuto S, Yoshida S, Jang JC (2003) Sterols regulate development and gene expression in Arabidopsis. Plant Physiol **131:** 1258–1269

Hemmerlin A, Harwood JL, Bach TJ (2012) A raison d'être for two distinct pathways in the early steps of plant isoprenoid biosynthesis? Prog Lipid Res **51:** 95–148

Hindt MN, Guerinot ML (2012) Getting a sense for signals: regulation of the plant iron deficiency response. Biochim Biophys Acta **1823:** 1521–1530

Hirooka K, Bamba T, Fukusaki E, Kobayashi A (2003) Cloning and kinetic characterization of Arabidopsis thaliana solanesyl diphosphate synthase. Biochem J **370:** 679–686

Hodzic A, Rappolt M, Amenitsch H, Laggner P, Pabst G (2008) Differential modulation of membrane structure and fluctuations by plant sterols and cholesterol. Biophys J **94:** 3935–3944

Hong SM, Bahn SC, Lyu A, Jung HS, Ahn JH (2010) Identification and testing of superior reference genes for a starting pool of transcript normalization in Arabidopsis. Plant Cell Physiol **51:** 1694–1706

Horvath DP, McLarney BK, Thomashow MF (1993) Regulation of *Arabidopsis thaliana* L. (Heynh) *cor78* in response to low temperature. Plant Physiol **103:** 1047–1053

Horvath SE, Daum G (2013) Lipids of mitochondria. Prog Lipid Res **52:** 590–614

Hosogaya N, Miyazaki T, Nagi M, Tanabe K, Minematsu A, Nagayoshi Y, Yamauchi S, Nakamura S, Imamura Y, Izumikawa K, et al (2013) The heme-binding protein Dap1 links iron homeostasis to azole resistance via the P450 protein Erg11 in Candida glabrata. FEMS Yeast Res **13:** 411–421

Hsieh FL, Chang TH, Ko TP, Wang AH (2011) Structure and mechanism of an Arabidopsis medium/long-chain-length prenyl pyrophosphate synthase. Plant Physiol **155:** 1079–1090

Huchelmann A, Brahim MS, Gerber E, Tritsch D, Bach TJ, Hemmerlin A (2016) Farnesol-mediated shift in the metabolic origin of prenyl groups used for protein prenylation in plants. Biochimie **127:** 95–102

Hugly S, McCourt P, Browse J, Patterson GW, Somerville C (1990) A chilling sensitive mutant of Arabidopsis with altered steryl-ester metabolism. Plant Physiol **93:** 1053–1062

Ischebeck T, Zbierzak AM, Kanwischer M, Dörmann P (2006) A salvage pathway for phytol metabolism in Arabidopsis. J Biol Chem **281:** 2470–2477

Ishiguro S, Nishimori Y, Yamada M, Saito H, Suzuki T, Nakagawa T, Miyake H, Okada K, Nakamura K (2010) The Arabidopsis FLAKY POLLEN1 gene encodes a 3-hydroxy-3-methylglutaryl-coenzyme A synthase required for development of tapetum-specific organelles and fertility of pollen grains. Plant Cell Physiol **51:** 896–911

Jang JC, Fujioka S, Tasaka M, Seto H, Takatsuto S, Ishii A, Aida M, Yoshida S, Sheen J (2000) A critical role of sterols in embryonic patterning and meristem programming revealed by the fackel mutants of Arabidopsis thaliana. Genes Dev **14:** 1485–1497

Jin H, Song Z, Nikolau BJ (2012) Reverse genetic characterization of two paralogous acetoacetyl CoA thiolase genes in Arabidopsis reveals their importance in plant growth and development. Plant J **70:** 1015–1032

Jones MO, Perez-Fons L, Robertson FP, Bramley PM, Fraser PD (2013) Functional characterization of long-chain prenyl diphosphate synthases from tomato. Biochem J **449:** 729–740

Keim V, Manzano D, Fernández FJ, Closa M, Andrade P, Caudepón D, Bortolotti C, Vega MC, Arró M, Ferrer A (2012) Characterization of Arabidopsis FPS isozymes and FPS gene expression analysis provide insight into the biosynthesis of isoprenoid precursors in seeds. PLoS ONE **7:** e49109

Kessler F, Glauser G (2014) Prenylquinone profiling in whole leaves and chloroplast subfractions. Methods Mol Biol **1153:** 213–226

Khan MS, Tawaraya K, Sekimoto H, Koyama H, Kobayashi Y, Murayama T, Chuba M, Kambayashi M, Shiono Y, Uemura M, et al (2009) Relative abundance of Delta(5)-sterols in plasma membrane lipids of root-tip cells correlates with aluminum tolerance of rice. Physiol Plant **135:** 73–83

Kim HB, Lee H, Oh CJ, Lee HY, Eum HL, Kim HS, Hong YP, Lee Y, Choe S, An CS, et al (2010) Postembryonic seedling lethality in the sterol-deficient Arabidopsis *cyp51A2* mutant is partially mediated by the composite action of ethylene and reactive oxygen species. Plant Physiol **152:** 192–205

Kim HB, Schaller H, Goh CH, Kwon M, Choe S, An CS, Durst F, Feldmann KA, Feyereisen R (2005) Arabidopsis *cyp51* mutant shows postembryonic seedling lethality associated with lack of membrane integrity. Plant Physiol **138:** 2033–2047

Kim J, Chang C, Tucker ML (2015) To grow old: regulatory role of ethylene and jasmonic acid in senescence. Front Plant Sci **6:** 20

Koo JC, Asurmendi S, Bick J, Woodford-Thomas T, Beachy RN (2004) Ecdysone agonist-inducible expression of a coat protein gene from tobacco mosaic virus confers viral resistance in transgenic Arabidopsis. Plant J **37:** 439–448

Kopischke M, Westphal L, Schneeberger K, Clark R, Ossowski S, Wewer V, Fuchs R, Landtag J, Hause G, Dörmann P, et al (2013) Impaired sterol ester synthesis alters the response of Arabidopsis thaliana to Phytophthora infestans. Plant J **73:** 456–468

Kumar MSS, Ali K, Dahuja A, Tyagi A (2015) Role of phytosterols in drought stress tolerance in rice. Plant Physiol Biochem **96:** 83–89

Kumari S, Priya P, Misra G, Yadav G (2013) Structural and biochemical perspectives in plant isoprenoid biosynthesis. Phytochem Rev **12:** 255–291

Laby RJ, Kim D, Gibson SI (2001) The *ram1* mutant of Arabidopsis exhibits severely decreased β-amylase activity. Plant Physiol **127:** 1798–1807

Langmead B, Salzberg SL (2012) Fast gapped-read alignment with Bowtie 2. Nat Methods **9:** 357–359

Langmead B, Trapnell C, Pop M, Salzberg SL (2009) Ultrafast and memory-efficient alignment of short DNA sequences to the human genome. Genome Biol **10:** R25

Leivar P, Antolín-Llovera M, Ferrero S, Closa M, Arró M, Ferrer A, Boronat A, Campos N (2011) Multilevel control of *Arabidopsis* 3-hydroxy-3-methylglutaryl coenzyme A reductase by protein phosphatase 2A. Plant Cell **23:** 1494–1511

Lenucci MS, Serrone L, De Caroli M, Fraser PD, Bramley PM, Piro G, Dalessandro G (2012) Isoprenoid, lipid, and protein contents in intact plastids isolated from mesocarp cells of traditional and high-pigment tomato cultivars at different ripening stages. J Agric Food Chem **60:** 1764–1775

Li J, Chory J (1997) A putative leucine-rich repeat receptor kinase involved in brassinosteroid signal transduction. Cell **90:** 929–938

Li R, Sun R, Hicks GR, Raikhel NV (2015) Arabidopsis ribosomal proteins control vacuole trafficking and developmental programs through the regulation of lipid metabolism. Proc Natl Acad Sci USA **112:** E89–E98

Lichtenthaler HK (1987) Chlorophyll and carotenoids: pigments of photosynthetic biomembranes. Methods Enzymol **148:** 350–382

Livak KJ, Schmittgen TD (2001) Analysis of relative gene expression data using real-time quantitative PCR and the 2(-Delta Delta C(T)) method. Methods **25:** 402–408

Lu W, Tang X, Huo Y, Xu R, Qi S, Huang J, Zheng C, Wu CA (2012) Identification and characterization of fructose 1,6-bisphosphate aldolase genes in Arabidopsis reveal a gene family with diverse responses to abiotic stresses. Gene **503:** 65–74

Lu Y, Zhou W, Wei L, Li J, Jia J, Li F, Smith SM, Xu J (2014) Regulation of the cholesterol biosynthetic pathway and its integration with fatty acid biosynthesis in the oleaginous microalga Nannochloropsis oceanica. Biotechnol Biofuels **7:** 81

Lundquist PK, Poliakov A, Giacomelli L, Friso G, Appel M, McQuinn RP, Krasnoff SB, Rowland E, Ponnala L, Sun Q, et al (2013) Loss of plastoglobule kinases ABC1K1 and ABC1K3 causes conditional degreening, modified prenyl-lipids, and recruitment of the jasmonic acid pathway. Plant Cell **25:** 1818–1839

Manzano D, Busquets A, Closa M, Hoyerová K, Schaller H, Kamínek M, Arró M, Ferrer A (2006) Overexpression of farnesyl diphosphate synthase in Arabidopsis mitochondria triggers light-dependent lesion formation and alters cytokinin homeostasis. Plant Mol Biol **61:** 195–213

Manzano D, Fernández-Busquets X, Schaller H, González V, Boronat A, Arró M, Ferrer A (2004) The metabolic imbalance underlying lesion formation in Arabidopsis thaliana overexpressing farnesyl diphosphate synthase (isoform 1S) leads to oxidative stress and is triggered by the developmental decline of endogenous HMGR activity. Planta **219:** 982–992

Martin VJJ, Pitera DJ, Withers ST, Newman JD, Keasling JD (2003) Engineering a mevalonate pathway in Escherichia coli for production of terpenoids. Nat Biotechnol **21:** 796–802

Martinis J, Kessler F, Glauser G (2011) A novel method for prenylquinone profiling in plant tissues by ultra-high pressure liquid chromatography-mass spectrometry. Plant Methods **7:** 23

Masferrer A, Arró M, Manzano D, Schaller H, Fernández-Busquets X, Moncaleán P, Fernández B, Cunillera N, Boronat A, Ferrer A (2002) Overexpression of Arabidopsis thaliana farnesyl diphosphate synthase (FPS1S) in transgenic Arabidopsis induces a cell death/senescence-like response and reduced cytokinin levels. Plant J **30:** 123–132

Mehrshahi P, Johnny C, DellaPenna D (2014) Redefining the metabolic continuity of chloroplasts and ER. Trends Plant Sci **19:** 501–507

Men S, Boutté Y, Ikeda Y, Li X, Palme K, Stierhof YD, Hartmann MA, Moritz T, Grebe M (2008) Sterol-dependent endocytosis mediates post-cytokinetic acquisition of PIN2 auxin efflux carrier polarity. Nat Cell Biol **10:** 237–244

Moeller CH, Mudd JB (1982) Localization of filipin-sterol complexes in the membranes of *Beta vulgaris* roots and *Spinacia oleracea* chloroplasts. Plant Physiol **70:** 1554–1561

Morikawa T, Mizutani M, Aoki N, Watanabe B, Saga H, Saito S, Oikawa A, Suzuki H, Sakurai N, Shibata D, et al (2006) Cytochrome P450 CYP710A encodes the sterol C-22 desaturase in *Arabidopsis* and tomato. Plant Cell **18:** 1008–1022

Nagata N, Suzuki M, Yoshida S, Muranaka T (2002) Mevalonic acid partially restores chloroplast and etioplast development in Arabidopsis lacking the non-mevalonate pathway. Planta **216:** 345–350

Nagel R, Bernholz C, Vranová E, Košuth J, Bergau N, Ludwig S, Wessjohann L, Gershenzon J, Tissier A, Schmidt A (2015) Arabidopsis thaliana isoprenyl diphosphate synthases produce the C25 intermediate geranylfarnesyl diphosphate. Plant J **84:** 847–859

Nechushtai R, Conlan AR, Harir Y, Song L, Yogev O, Eisenberg-Domovich Y, Livnah O, Michaeli D, Rosen R, Ma V, et al (2012) Characterization of *Arabidopsis* NEET reveals an ancient role for NEET proteins in iron metabolism. Plant Cell **24:** 2139–2154

Nieto B, Forés O, Arró M, Ferrer A (2009) Arabidopsis 3-hydroxy-3-methylglutaryl-CoA reductase is regulated at the post-translational level in response to alterations of the sphingolipid and the sterol biosynthetic pathways. Phytochemistry **70:** 53–59

Nogales-Cadenas R, Carmona-Saez P, Vazquez M, Vicente C, Yang X, Tirado F, Carazo JM, Pascual-Montano A (2009) GeneCodis: interpreting gene lists through enrichment analysis and integration of diverse biological information. Nucleic Acids Res **37:** W317–W322

Nordin K, Heino P, Palva ET (1991) Separate signal pathways regulate the expression of a low-temperature-induced gene in Arabidopsis thaliana (L.) Heynh. Plant Mol Biol **16:** 1061–1071

Ohnuma S, Koyama T, Ogura K (1992) Chain length distribution of the products formed in solanesyl diphosphate synthase reaction. J Biochem **112:** 743–749

Opitz S, Nes WD, Gershenzon J (2014) Both methylerythritol phosphate and mevalonate pathways contribute to biosynthesis of each of the major isoprenoid classes in young cotton seedlings. Phytochemistry **98:** 110–119

Ossowski S, Schwab R, Weigel D (2008) Gene silencing in plants using artificial microRNAs and other small RNAs. Plant J **53:** 674–690

Padidam M, Gore M, Lu DL, Smirnova O (2003) Chemical-inducible, ecdysone receptor-based gene expression system for plants. Transgenic Res **12:** 101–109

Pan JJ, Kuo TH, Chen YK, Yang LW, Liang PH (2002) Insight into the activation mechanism of Escherichia coli octaprenyl pyrophosphate synthase derived from pre-steady-state kinetic analysis. Biochim Biophys Acta **1594:** 64–73

Pollier J, Moses T, González-Guzmán M, De Geyter N, Lippens S, Vanden Bossche R, Marhavý P, Kremer A, Morreel K, Guérin CJ, et al (2013) The protein quality control system manages plant defence compound synthesis. Nature **504:** 148–152

Posé D, Castanedo I, Borsani O, Nieto B, Rosado A, Taconnat L, Ferrer A, Dolan L, Valpuesta V, Botella MA (2009) Identification of the Arabidopsis dry2/sqe1-5 mutant reveals a central role for sterols in drought tolerance and regulation of reactive oxygen species. Plant J **59:** 63–76

Poulter CD (2006) Farnesyl diphosphate synthase: a paradigm for understanding structure and function relationships in E-polyprenyl diphosphate synthases. Phytochem Rev **5:** 17–26

Qian P, Han B, Forestier E, Hu Z, Gao N, Lu W, Schaller H, Li J, Hou S (2013) Sterols are required for cell-fate commitment and maintenance of the stomatal lineage in Arabidopsis. Plant J **74:** 1029–1044

Roche Y, Gerbeau-Pissot P, Buhot B, Thomas D, Bonneau L, Gresti J, Mongrand S, Perrier-Cornet JM, Simon-Plas F (2008) Depletion of phytosterols from the plant plasma membrane provides evidence for disruption of lipid rafts. FASEB J **22:** 3980–3991

Rodríguez-Celma J, Pan IC, Li W, Lan P, Buckhout TJ, Schmidt W (2013) The transcriptional response of Arabidopsis leaves to Fe deficiency. Front Plant Sci **4:** 276

Rodríguez-Concepción M, Forés O, Martinez-García JF, González V, Phillips MA, Ferrer A, Boronat A (2004) Distinct light-mediated pathways regulate the biosynthesis and exchange of isoprenoid precursors during *Arabidopsis* seedling development. Plant Cell **16:** 144–156

Ryder NS (1992) Terbinafine: mode of action and properties of the squalene epoxidase inhibition. Br J Dermatol (Suppl 39) **126:** 2–7

Schaeffer A, Bronner R, Benveniste P, Schaller H (2001) The ratio of campesterol to sitosterol that modulates growth in Arabidopsis is controlled by STEROL METHYLTRANSFERASE 2;1. Plant J **25:** 605–615

Schaller H (2003) The role of sterols in plant growth and development. Prog Lipid Res **42:** 163–175

Schrick K, Debolt S, Bulone V (2012) Deciphering the molecular functions of sterols in cellulose biosynthesis. Front Plant Sci **3:** 84

Schrick K, Mayer U, Horrichs A, Kuhnt C, Bellini C, Dangl J, Schmidt J, Jürgens G (2000) FACKEL is a sterol C-14 reductase required for organized cell division and expansion in Arabidopsis embryogenesis. Genes Dev **14:** 1471–1484

Schrick K, Mayer U, Martin G, Bellini C, Kuhnt C, Schmidt J, Jürgens G (2002) Interactions between sterol biosynthesis genes in embryonic development of Arabidopsis. Plant J **31:** 61–73

Schuler I, Milon A, Nakatani Y, Ourisson G, Albrecht AM, Benveniste P, Hartman MA (1991) Differential effects of plant sterols on water permeability and on acyl chain ordering of soybean phosphatidylcholine bilayers. Proc Natl Acad Sci USA **88:** 6926–6930

Schwab R, Ossowski S, Riester M, Warthmann N, Weigel D (2006) Highly specific gene silencing by artificial microRNAs in *Arabidopsis*. Plant Cell **18:** 1121–1133

Seltmann MA, Hussels W, Berger S (2010a) Jasmonates during senescence: signals or products of metabolism? Plant Signal Behav **5:** 1493–1496

Seltmann MA, Stingl NE, Lautenschlaeger JK, Krischke M, Mueller MJ, Berger S (2010b) Differential impact of lipoxygenase 2 and jasmonates on natural and stress-induced senescence in Arabidopsis. Plant Physiol **152:** 1940–1950

Sengupta D, Naik D, Reddy AR (2015) Plant aldo-keto reductases (AKRs) as multi-tasking soldiers involved in diverse plant metabolic processes and stress defense: A structure-function update. J Plant Physiol **179:** 40–55

Senthil-Kumar M, Wang K, Mysore KS (2013) AtCYP710A1 gene-mediated stigmasterol production plays a role in imparting temperature stress tolerance in Arabidopsis thaliana. Plant Signal Behav **8:** e23142

Sewelam N, Jaspert N, Van Der Kelen K, Tognetti VB, Schmitz J, Frerigmann H, Stahl E, Zeier J, Van Breusegem F, Maurino VG (2014) Spatial H_2O_2 signaling specificity: H_2O_2 from chloroplasts and peroxisomes modulates the plant transcriptome differentially. Mol Plant **7:** 1191–1210

Shin R, Berg RH, Schachtman DP (2005) Reactive oxygen species and root hairs in Arabidopsis root response to nitrogen, phosphorus and potassium deficiency. Plant Cell Physiol **46:** 1350–1357

Singh AK, Dwivedi V, Rai A, Pal S, Reddy SGE, Rao DKV, Shasany AK, Nagegowda DA (2015) Virus-induced gene silencing of Withania somnifera squalene synthase negatively regulates sterol and defence-related genes resulting in reduced withanolides and biotic stress tolerance. Plant Biotechnol J **13:** 1287–1299

Sivy TL, Fall R, Rosenstiel TN (2011) Evidence of isoprenoid precursor toxicity in Bacillus subtilis. Biosci Biotechnol Biochem **75:** 2376–2383

Soler E, Clastre M, Bantignies B, Marigo G, Ambid C (1993) Uptake of isopentenyl diphosphate by plastids isolated from Vitis vinifera L. cell suspensions. Planta **191:** 324–329

Souter M, Topping J, Pullen M, Friml J, Palme K, Hackett R, Grierson D, Lindsey K (2002) *hydra* mutants of *Arabidopsis* are defective in sterol profiles and auxin and ethylene signaling. Plant Cell **14:** 1017–1031

Suzuki M, Kamide Y, Nagata N, Seki H, Ohyama K, Kato H, Masuda K, Sato S, Kato T, Tabata S, et al (2004) Loss of function of 3-hydroxy-3-methylglutaryl coenzyme A reductase 1 (HMG1) in Arabidopsis leads to

dwarfing, early senescence and male sterility, and reduced sterol levels. Plant J **37:** 750–761

Suzuki M, Nakagawa S, Kamide Y, Kobayashi K, Ohyama K, Hashinokuchi H, Kiuchi R, Saito K, Muranaka T, Nagata N (2009) Complete blockage of the mevalonate pathway results in male gametophyte lethality. J Exp Bot **60:** 2055–2064

Tholl D, Lee S (2011) Terpene specialized metabolism in Arabidopsis thaliana. The Arabidopsis Book **9:** e0143, doi/10.1043/tab.0143

Thomas E, Roman E, Claypool S, Manzoor N, Pla J, Panwar SL (2013) Mitochondria influence CDR1 efflux pump activity, Hog1-mediated oxidative stress pathway, iron homeostasis, and ergosterol levels in Candida albicans. Antimicrob Agents Chemother **57:** 5580–5599

Trapnell C, Hendrickson DG, Sauvageau M, Goff L, Rinn JL, Pachter L (2013) Differential analysis of gene regulation at transcript resolution with RNA-seq. Nat Biotechnol **31:** 46–53

Trapnell C, Pachter L, Salzberg SL (2009) TopHat: discovering splice junctions with RNA-Seq. Bioinformatics **25:** 1105–1111

Trapnell C, Williams BA, Pertea G, Mortazavi A, Kwan G, van Baren MJ, Salzberg SL, Wold BJ, Pachter L (2010) Transcript assembly and quantification by RNA-Seq reveals unannotated transcripts and isoform switching during cell differentiation. Nat Biotechnol **28:** 511–515

Urbany C, Benke A, Marsian J, Huettel B, Reinhardt R, Stich B (2013) Ups and downs of a transcriptional landscape shape iron deficiency associated chlorosis of the maize inbreds B73 and Mo17. BMC Plant Biol **13:** 213

Vandermoten S, Haubruge E, Cusson M (2009) New insights into short-chain prenyltransferases: structural features, evolutionary history and potential for selective inhibition. Cell Mol Life Sci **66:** 3685–3695

Varkonyi-Gasic E, Wu R, Wood M, Walton EF, Hellens RP (2007) A highly sensitive RT-PCR method for detection and quantification of microRNAs. Plant Methods **3:** 12

Vasicek EM, Berkow EL, Flowers SA, Barker KS, Rogers PD (2014) UPC2 is universally essential for azole antifungal resistance in Candida albicans. Eukaryot Cell **13:** 933–946

Vom Dorp K, Hölzl G, Plohmann C, Eisenhut M, Abraham M, Weber APM, Hanson AD, Dörmann P (2015) Remobilization of phytol from chlorophyll degradation is essential for tocopherol synthesis and growth of *Arabidopsis*. Plant Cell **27:** 2846–2859

Vranová E, Coman D, Gruissem W (2012) Structure and dynamics of the isoprenoid pathway network. Mol Plant **5:** 318–333

Vranová E, Coman D, Gruissem W (2013) Network analysis of the MVA and MEP pathways for isoprenoid synthesis. Annu Rev Plant Biol **64:** 665–700

Wagatsuma T, Khan MS, Watanabe T, Maejima E, Sekimoto H, Yokota T, Nakano T, Toyomasu T, Tawaraya K, Koyama H, et al (2015) Higher sterol content regulated by CYP51 with concomitant lower phospholipid content in membranes is a common strategy for aluminium tolerance in several plant species. J Exp Bot **66:** 907–918

Wang H, Nagegowda DA, Rawat R, Bouvier-Navé P, Guo D, Bach TJ, Chye ML (2012a) Overexpression of Brassica juncea wild-type and mutant HMG-CoA synthase 1 in Arabidopsis up-regulates genes in sterol biosynthesis and enhances sterol production and stress tolerance. Plant Biotechnol J **10:** 31–42

Wang K, Senthil-Kumar M, Ryu CM, Kang L, Mysore KS (2012b) Phytosterols play a key role in plant innate immunity against bacterial pathogens by regulating nutrient efflux into the apoplast. Plant Physiol **158:** 1789–1802

Wang KC, Ohnuma S (2000) Isoprenyl diphosphate synthases. Biochim Biophys Acta **1529:** 33–48

Wang Z, Benning C (2012) Chloroplast lipid synthesis and lipid trafficking through ER-plastid membrane contact sites. Biochem Soc Trans **40:** 457–463

Wasternack C, Hause B (2013) Jasmonates: biosynthesis, perception, signal transduction and action in plant stress response, growth and development. An update to the 2007 review in Annals of Botany. Ann Bot (Lond) **111:** 1021–1058

Wentzinger LF, Bach TJ, Hartmann M-A (2002) Inhibition of squalene synthase and squalene epoxidase in tobacco cells triggers an up-regulation of 3-hydroxy-3-methylglutaryl coenzyme A reductase. Plant Physiol **130:** 334–346

Whitaker BD (1994) Lipid changes in mature-green tomatoes during ripening, during chilling, and after rewarming subsequent to chilling. J Am Soc Hortic Sci **119:** 994–999

Yalovsky S, Kulukian A, Rodríguez-Concepción M, Young CA, Gruissem W (2000) Functional requirement of plant farnesyltransferase during development in *Arabidopsis*. Plant Cell **12:** 1267–1278

Zhang H, Ohyama K, Boudet J, Chen Z, Yang J, Zhang M, Muranaka T, Maurel C, Zhu JK, Gong Z (2008) Dolichol biosynthesis and its effects on the unfolded protein response and abiotic stress resistance in *Arabidopsis*. Plant Cell **20:** 1879–1898